Universität Ulm

Fakultät für Informatik

Recurrent V1 – V2 Interaction in Early Visual Boundary Processing

Heiko Neumann
Wolfgang Sepp
Universität Ulm

Nr. 98-10

Ulmer Informatik-Berichte

Dezember 1998

Recurrent V1 – V2 Interaction in Early Visual Boundary Processing[1]

Heiko Neumann and Wolfgang Sepp

Universität Ulm, Abt. Neuroinformatik, 89069 Ulm, Germany

(hneumann@neuro.informatik.uni-ulm.de)

Abstract

A majority of cortical areas are connected via feedforward and feedback fiber projections. In feedforward pathways we mainly observe stages of feature detection and integration. The computational role of the descending pathways at different stages of processing remains mainly unknown. Based on empirical findings we suggest that the *top-down feedback* pathways subserve a context dependent gain control mechanism. We propose a new computational model for recurrent contour processing in which normalized activities of orientation selective contrast cells are fed forward to the next higher processing stage. There, the arrangement of input activation is matched against local patterns of contour shape. The resulting activities are subsequently fed back to the previous stage to locally enhance those initial measurements that are consistent with the top-down generated responses. In all, we suggest a computational theory for recurrent processing in visual cortex in which the significance of local measurements is evaluated on the basis of a broader visual context that is represented in terms of contour code patterns. The model serves as a framework to link physiological with perceptual data gathered in psychophysical experiments. It handles a variety of perceptual phenomena, such as e.g. the local grouping of fragmented shape outline, texture surround and density effects, and the interpolation of illusory contours.

1 Motivation

The brain is steadily confronted with a massive information flow that arrives via several sensory channels. In vision, pattern arrangements that signal coherent surface quantities must be somehow reliably detected and grouped into elementary items. Such a grouping enables the segregation of figural components from cluttered background as well as the adaptive focussing of processing capacities while suppressing unimportant parts of the scene (Crick, 1984; Grossberg, 1980).

A characteristic feature of the cortical architecture is that the majority of (visual) cortical areas are linked bidirectionally by feedforward and feedback fiber projections. So far, the precise computational role of the descending feedback pathways at different stages of processing remains largely unknown. Previous computational models incorporate feedback mechanisms to complete initially fragmented contours (Grossberg and Mingolla, 1985), or, more recently, to carry top-down

[1]This research is supported in part by a University grant "Neue Pools" (TG 98, no. 427 98). Part of the research work by H.N. is performed in the Collaborative Research Center on the "*Integration of symbolic and subsymbolic information processing in adaptive sensory-motor systems*" (SFB-527), which is located at the Univ. of Ulm and is funded by the German Science Foundation (DFG).

shape templates to generate the representation of residuals from the difference between templates and the sensory input (Mumford, 1991, 1994). A comprehensive discussion of these and other approaches is given in Section 5.

Recent empirical evidence supports the view that top-down projections primarily serve as a modulation mechanism to control the responsiveness of cells in primary visual cortex (Lamme, 1995; Salin and Bullier, 1995). Based on these findings our model proposes computational principles of feedforward and feedback interaction between a pair of cortical areas. In the lower area mechanisms of local feature or signal detection process the input whereas in the higher area these local measurements are integrated and matched against model information, or priors, of coarse shape outline. By way of recurrent projection these activities feed a gain control mechanism to selectively enhance those initial estimates that are consistent with a broader visual context provided by the stimulus contour and shape outline. This facilitates the segmentation of surface layout and figure-ground segregation. Since, so far, no all-embracing neural theory of surface perception has been developed, the proposed model contributes to a better understanding of the general computational principles involved in grouping and surface segmentation. The model links physiology and psychophysics, incorporating empirical data from both research directions, and provides a common framework for distinct perceptual phenomena.

2 Summary of Empirical Findings

The computational model proposed here has the following key components: *feedforward* and *feedback* processing between a pair of model areas, localized receptive field processing, lateral competitive interaction, and lateral horizontal integration within areas. Empirical evidence is widespread and not entirely coherent. In order to justify the computational stages of the model we review recent physiological and morphological findings specifically emphasizing data about cortico-cortical *feedback* processing. This summary is accompanied by recent psychophysical data on spatial grouping and interpolation that relates to broader visual contexts integrating localized measures.

Morphology and Physiology. The majority of areas in the cortex is connected in a bidirectional fashion. Thus, for pairs of areas mostly a forward as well as a backward stream can be identified. The functional role of the feedback stream in the reciprocal wiring between areas is not yet clearly established. This holds also for V1–V2, the focus of our interest in this contribution. Feedforward projections from monkey V1 selectively couple cells within separate processing streams, e.g. for form, color and motion/depth (DeYoe and Van Essen, 1988). The pattern of feedback connectivity shows a precise retinotopic correspondence, however, the reciprocated connections di-

verge from V2 to multiple clusters in V1 (Rockland and Virga, 1989) and possibly enhance the integration of visual information across different channels (Krubitzer and Kaas, 1989). Whether this is due to intrinsic divergent backprojection is not entirely clear. It has been concluded that indirect effects reflecting the convergence of information flow within V2 could also be the underlying reason for the substantial divergence (Rockland and Virga, 1989). In cat, Bullier *et al.* (1988) found that feedback connectivity to area 17 from sites in area 18 and 19 is in precise retinotopic correspondence. Thus, the V1–V2 reciprocity may indeed be mainly guided by a point-to-point connectivity scheme as it was suggested for the linking of cells in cytochrome oxidase blobs and bands (Livingstone and Hubel, 1984). Concerning the processing of visual form information, it has been shown that V1–V2 forward connections link patches of similar orientation selectivity (Gilbert and Wiesel, 1989). Receptive field sizes in V2 are substantially larger than those in V1 (von der Heydt *et al.*, 1993). Horizontal connections of oriented V2 cells link targets of a wide range of orientation preference but avoid those with orthogonal orientations (Malach *et al.*, 1994). Thus, one can conclude that the structure of the wiring scheme supports the specificity of contrast orientation and curved shape outline.

Several physiological studies (with monkey and cat) indicate that activation of the V2 feedback pathway is primarily excitatory and acts to *modulate* the output of striate cortex (Salin and Bullier, 1995). Feedback activation alone is not sufficient to drive V1 neurones if they are not stimulated by a visual feeding input (Sandell and Schiller, 1982). Inactivation of area V2 reduces V1 cell responsiveness while leaving orientation and direction selectivity unimpaired (Sandell and Schiller, 1982; Mignard and Malpeli, 1991). It is thus believed that the modulation is excitatory such that feedback enhances activity of V1 neurones (Sandell and Schiller, 1982; Salin and Bullier, 1995). Further evidence is gained by recent studies on figure-ground segregation. For static orientation patterns as well as motion displays cell activities in monkey V1 are modulated in a context-dependent way (Lamme *et al.*, 1997). The modulation is abolished when the animal is anaesthesized (Zipser *et al.*, 1997). Structure detected in higher-order areas contributes to the context-sensitive regulation of activity in a lower area such that activity modulation serves as a general mechanism for figure-ground segregation already at the early stage of V1 and V2 processing (Lamme, 1995).

The modulatory influence of visual context on the response of a target cell to an individual stimulus element has also been demonstrated. V1 cell responses to isolated optimally oriented bars are reduced if the bar is supplemented by a texture of oriented bars of the same type. Reduction is maximal for a texture defined by bars of same orientation as in the center, weaker reduction is observed for randomly oriented bars, and even weaker effects occur for a surround pattern

with orthogonally oriented bars (Knierim and VanEssen, 1992). Cell responses are raised again – even beyond the level of individual stimulation – if the central element is supplied by colinearly arranged co-oriented flanking items while keeping the surround texture. The aligned bars define a perceptually salient contour segment and "pop-out" pre-attentively (Knierim and VanEssen, 1992; Kapadia *et al.*, 1995).

The integration or grouping of aligned items requires a mechanism of long-range interaction between oriented contrasts. Candidate mechanisms are V2 contour cells which respond to oriented contrast stimuli as well as to illusory contours of the same orientation (von der Heydt *et al.*, 1984). The magnitude of response for illusory contours in line gratings increases monotonically with increased line density of gratings. A contour cell can be maximally excited by a physical contrast such as a bar (von der Heydt and Peterhans, 1989). Such a gradual variation indicates that the strength of the feeding input mainly determines the contour cell response instead of an all-or-none classification of coherent input. V2 contour neurons have been probed with illusory-bar stimuli. They selectively respond to coherent arrangements having both half-figures of an illusory bar intact. If one half is missing the cell response drops to the level of spontaneous activity (Peterhans and von der Heydt, 1989). This suggests that V2 contour cells signal the presence of locally coherent stimulus patterns where the reponse to the whole is greater than the sum of responses to individual pattern items.

Psychophysics. Perceptual organization is an elementary principle to achieve figure-ground segregation and surface segmentation. The underlying perception of various grouping phenomena have been investigated in order to understand the encoding of spatial information. Different morphologies in random dot interference patterns have been studied in Glass patterns (Glass and Pérez, 1973). The detectability of local dot correlations has been suggested to be facilitated by local cortical line detectors (Hubel and Wiesel, 1968) whereas the global integration might rely on neural pattern recognition mechanisms (Glass, 1969). Several authors (e.g. Smits *et al.*, 1985) suggested that dot-patterns are grouped on the basis of proximity that can be measured by directionally weighted averaging, or low-pass filtering. However, the introduction of 'energy' differences in feature-pair items, the inversion of contrast polarity, and the use of triple-dot items allows to disrupt a coherent perception of Glass patterns (Prazdny, 1984, 1986). These effects indicate that more complex local mechanisms are involved in order to explain the results. Prazdny (1986) conjectured that local non-linear mechanisms may be supplied by top-down mechanisms. A study by Sagi and Kovaćs (1993) confirmed the contribution of a process which involves oriented long range interactions. The detection of spatial arrangements of oriented Gabor patches within a field of distractors is facilitated by target elements which are placed and oriented along the

path-axis in the grouping direction (Field *et al.*, 1993; Polat and Sagi,1994). Kapadia *et al.* (1995) systematically investigated contrast threshold reduction effects for target line detection. The distance along the axis of colinearity, displacement orthogonal to this axis and deviation in orientation where critical parameters for optimal placements of flanking bars. Spatial support could be disrupted through items that destroy feature discontinuity.

The strength of grouping line-like items (instead of dots) also depends on stimulus features such as edge alignment, orientation, length, and contrast magnitude (Beck *et al.*, 1989), but not on contrast polarity (Gilchrist *et al.*, 1997). Similar selectivities have been observed as critical for the visual interpolation in illusory contour perception (Kellman and Shipley, 1991; Prazdny, 1983; see the overview by Lesher, 1995). Surface segmentation and figure-ground segregation necessitates contour completion over gaps where fore-/background luminance differences are missing (Peterhans and von der Heydt, 1991). Consequently, contour completion depends on discontinuities (inducers) which are oriented in the direction of the interpolated contour. Completion occurs in the same direction as the inducing contrast as well as orthogonal to line endings (Kanizsa, 1976; Prazdny, 1983; Shipley and Kellman, 1990). Some authors claim that basic visual filtering at different spatial resolutions is the primarily mechanism for subjective contour perception (Ginsburg, 1987). However, this view is challenged by investigations using stimuli (Kanizsa squares) of same average luminance for figure and ground in which illusory figure brightening is abolished. Subjective contours remain robust which indicates causal effects of spatial configuration as the main feature (Kellman and Loukides, 1987). The strength of visual interpolation between edges depends on the ratio of physical edge (inducer) length to total contour length (Shipley and Kellman, 1992). Such a mechanism is ecologically valuable since the formation of perceptual units remains invariant under changing viewing distances. This indicates that illusory contour generation is related to surface segmentation that cannot be simply explained by spatial filtering.

In all, a rich set of properties for perceptual contour and unit formation has been identified. Specific local features in stimulus configurations initiate the integration into coherent percepts. The more global mechanisms evaluate the arrangement of local responses according to relatable stimulus properties. The local effects of feature detection can already be linked to neural mechanisms such as simple and complex cell processing. Oriented long-range effects may be implemented neurally utilizing V1 horizontal intra-cortical connections. However, with such an early mechanism alone one falls short to explain completion, facilitation, and reduction effects that occur over ranges of 5 up to 8 deg. visual angle (von der Heydt *et al.*, 1993; Zipser *et al.*, 1996). Moreover, the cause of variations in the strength of perceptual contours depending on various local and global stimulus features remains unknown. Neither do we have a solid theory of neural mechanisms of surface

perception. Rather informal experiments highlight how local stimulus elements appear perceptually different depending on more global configurations and context. Barrow and Tenenbaum (1981) demonstrated how identical shading gradients represent different surface curvatures depending on changing shapes of object silhouettes. Similarly, Mumford (1994) showed how a given shading patch appears differently depending on the global surface arrangement. Perceptual elements can be absorbed by the structure of the whole such that a perceiver cannot even see it anymore (Kanizsa, 1968). This again indicates that more global aspects of visual stimuli influence local feature measurements. We suggest that recurrencies provide "... a plausible functional role for the ubiquitious feedback pathways in visual cortex, that of providing a broader context for the firing of cells in lower areas." (Knierim and Van Essen, 1992, p.978).

3 Computational Model

3.1 Functionality and Computational Mechanisms

We suggest that the variety of empirical findings can be explained within a framework of basic computational mechanisms. In the ascending processing stream local contrast orientation is initially measured by cells with oriented receptive fields (RF), such as cortical simple and complex cells. Thus, for a pair of bidirectionally connected cortical areas (V1 and V2 in our case) the "lower" area serves as a stage of feature measurement and signal detection. Activities from local measurements are subsequently contrast enhanced and normalized by a mechanism of divisive inhibition (Fig. 1, left & center; compare with Heeger, 1992 and Heeger *et al.*, 1996). The resulting activations are fed forward to the "higher" area where they are subsequently integrated by cells utilizing oriented long-range RF integration. Due to their increased RF size such an integration along an oriented path bridges gaps including those corresponding to perceived illusory contours. The effectivity of local integration is based on a multitude of stimulus features, such as relative spatial position, alignment, and local orientation. An arrangement of items in a spatial neighborhood of a target cell facilitate its response in a graded fashion. A significant contrast element in a particular configuration is likely to occur in conjunction with other items that are arranged curvilinearly. The effective weightings between the target location and other elements in a space/orientation neighborhood should encode the likelihood of occurrence of smooth stimulus shape segments. In other words, spatial weightings of V2 cells with oriented long-range selectivity represent "models" of visual entities, or local Gestalts, that frequently occur in regular visual form patterns (Fig. 1, right; compare with Grossberg and Mingolla, 1985, and Zucker, 1985 for first models of oriented space/orientation integration). The "higher" area locally matches "model templates" (or priors; see Mumford, 1994)

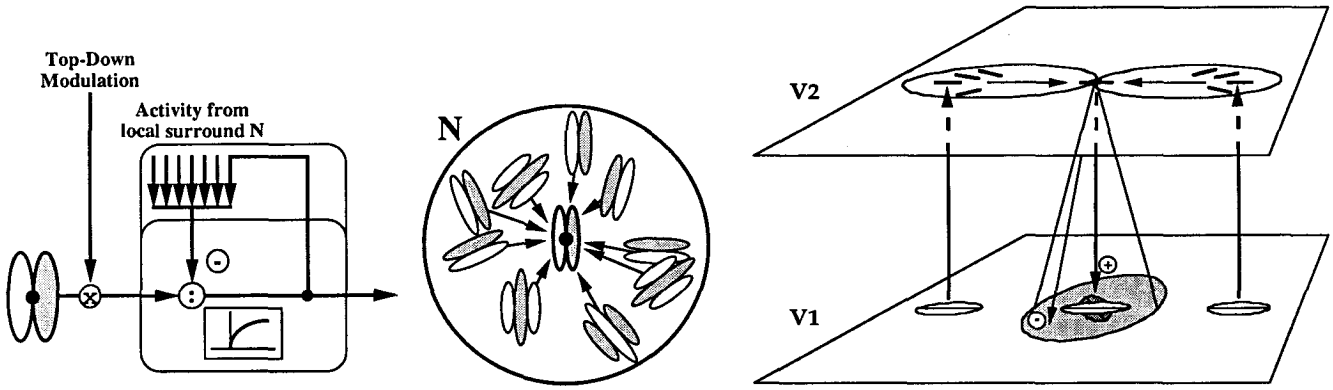

Figure 1: *Model components. Left and Center: Feeding input is processed by localized V1 cells with oriented receptive fields whose responses are modulated by top-down activation. Responses are subsequently normalized by a shunting competition among cells in a local neighborhood $\mathcal{N}$ (left figure modified after Heeger et al., 1996). Right: Model V2 cells resembling 'contour templates' integrate V1 activations from elongated branches. Once the cell is activated from both branches its activation is fed back to enhance activated contrast cells in V1 of matching orientation.*

of expected visual structure against the incoming data carried by the ascending pathway.

The matching process generates an activity pattern in the higher area that is propagated backwards via the descending feedback pathway. In V1 responses of cells that match position and orientation of activated V2 contour cells are selectively enhanced, those that do not are inhibited. Thus, any feedback activation signals the degree of consistency between local measurements and model expectations (Grossberg, 1980). Feedback is modulatory realizing an excitatory gain control mechanism that enhances already active cells in V1. The modulation is accompanied by competitive interactions to realize a "soft gating" mechanism that selectively filters activities corresponding to salient input arrangements while suppressing spurious signals that are inconsistent with the top-down priors or shape templates (Fig. 1, right).

3.2 Description of Mechanisms

We implemented the model architecture to demonstrate the functionality of interaction between areas V1 and V2. All network levels are modeled as consisting of single compartment cells with gradual saturation-type first-order activation dynamics. Subsequently, we present individual stages of processing that are denoted as follows: $c_{i\theta}$ is the output of initial oriented contrast detection at the level of cortical simple and complex cells in V1; $l_{i\theta}^{(1)}$ and $l_{i\theta}^{(2)}$ denote activities in the *lower* area (V1) for computational stages utilizing top-down modulation and contrast enhancement and normalization, respectively; $h_{i\theta}^{(1)}$ and $h_{i\theta}^{(2)}$ denote activities in the *higher* area (V2) resulting from integration of normalized contrast activation and subsequent normalization, respectively. Subscripts

i and θ denote spatial location and orientation, respectively.

Model V1. At the initial measurement stage of model area V1 input luminance stimuli are processed by oriented masks of local contrast direction resembling cortical simple cells (Hubel and Wiesel, 1968). We utilize linear simple cell models with odd-symmetric RF profiles for $K = 8$ different orientations, $\theta = k\frac{\pi}{K}$ with $k = 0, 1, .., K-1$. Responses of simple cells sensitive to opposite contrast polarity are subsequently pooled to generate complex cell responses, $c_{i\theta}$, selective to orientation but insensitive to local contrast polarity.

Complex cell responses are fed to a sequence of competitive interactions in model area V1, the first stage of which modulates the output of oriented contrast detection through feedback activation generated by V2 contour cells. This recurrent processing generates activities $l_{i\theta}^{(1)}$ by the following shunting interaction

$$\frac{\partial}{\partial t} l_{i\theta}^{(1)} = -\alpha_1 l_{i\theta}^{(1)} + \beta_1 c_{i\theta} \left(1 + C \left\{h^{(2)} \star \Psi^+\right\}_{i\theta}\right) - \zeta_1 l_{i\theta}^{(1)} \left\{h^{(2)} \star \Psi^- \star \Lambda^-\right\}_{i\theta}. \tag{1}$$

The constants α_1, β_1 and ζ_1 define the parameters of the dynamics of cell interaction, where α_1 determines the activity decay and β_1 and ζ_1 denote constant shunting parameters for excitatory and inhibitory response amplitudes, respectively. The constant C represents the gain factor of top-down modulation via V2 contour cell activations. Weighted averaging of activities is denoted by a convolution operation ($\star$) utilizing weighting functions Λ and Ψ in space and orientation domain, respectively. Excitatory and inhibitory interactions are denoted by '+' and '−', respectively.

Activities $h_{i\theta}^{(2)}$ denote feedback activations delivered by the descending pathway. Closer inspection of Eqn. 1 demonstrates that the enhancement via feedback activation is only effective at those positions with non-zero V1 complex cell response. Such a modulatory interaction is similar to the linking mechanism proposed by Eckhorn *et al.* (1990). The spatial shape and extent of inhibitory interaction follows a Gaussian distribution consistent with recent investigations by Kastner *et al.* (1996). In contrast to approaches such as of Grossberg and Mingolla (1985) and Grossberg *et al.* (1997) in our model no activity spreading or completion occurs for locations between inducing elements of a salient perceptual contour arrangement. Thus, here the computational competence of feedforward and feedback interaction is the context-sensitive selection and enhancement of early signal and feature measurements.

The top-down modulated activities subsequently undergo a second stage of shunting ON-center/OFF-surround competition between activities in a spatial and orientational neighborhood

$$l_{i\theta}^{(2)} = \frac{\beta_2 l_{i\theta}^{(1)} - \delta_2 \left\{l^{(1)} \star \Psi^- \star \Lambda^-\right\}_{i\theta}}{\alpha_2 + \zeta_2 \left\{l^{(1)} \star \Psi^- \star \Lambda^-\right\}_{i\theta}}, \tag{2}$$

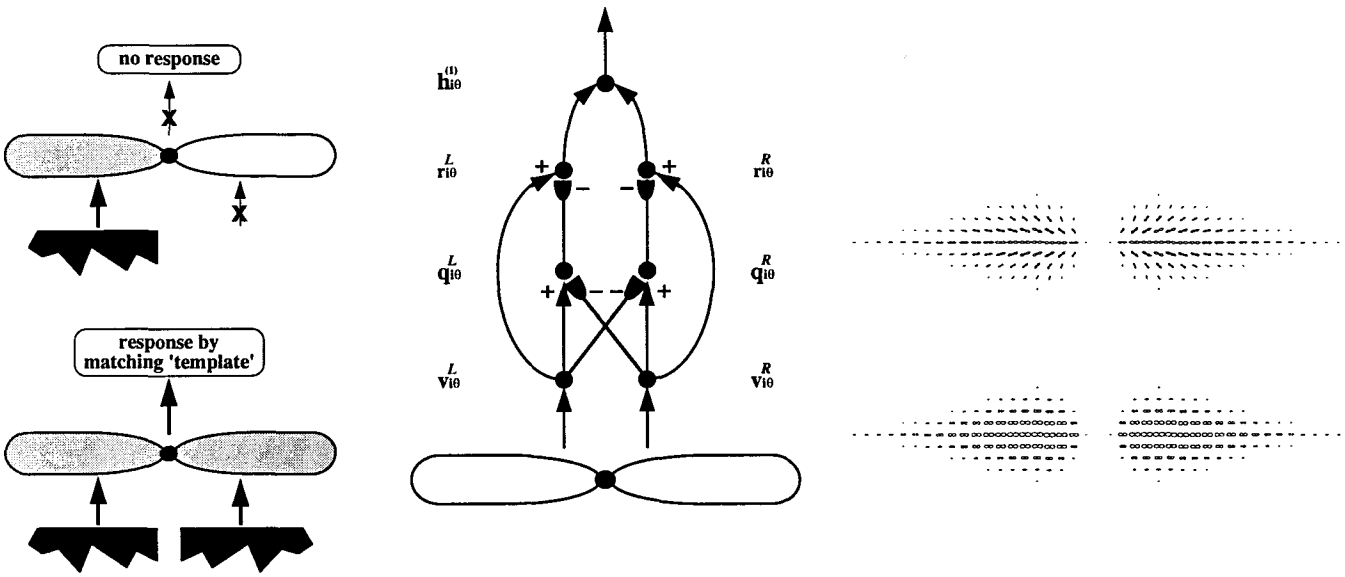

Figure 2: *Integration of input activation in position/orientation space utilizing contour cell RFs with bipole subfield organization. Left: No target cell response is elicited if forward input is supplied only from one side of the RF sampling (top), in order to get the target cell activated requires input from both input branches (bottom) (compare with the model proposed by [Grossberg and Mingolla, 1985] and the findings by [Peterhans and von der Heydt, 1989]). Center: Model circuit that implements the functionality of a V2 contour cell tuned to horizontal orientation $\theta = 0$. Three sub-stages process the input activation gathered from both branches before being integrated at the final stage to generate $h^{(1)}_{i\theta}$ responses (see text for details). Right: Display of the* ON *(top) and* OFF *(bottom) subfield components of elongated weighting functions of V2 contour cells.*

where α_2, β_2, δ_2, and ζ_2 are constants. With this competitive interaction the initial top-down modulated activities are contrast enhanced and normalized by subtractive and divisive inhibition. Together, simple-cell processing, enhancement, and subsequent normalization is consistent with recent experimental and theoretical work (DeAngelis *et al.*, 1993). Without incorporating any auxiliary compressive signal function, as suggested in other models (Heeger, 1992; Heeger *et al.*, 1996), model V1 cells generate locally normalized responses that have been selectively enhanced by a context dependent modulating input from cells in model V2 (Knierim and Van Essen, 1992). In all, the combination of both competitive processing stages in model V1 generating activities $l^{(1)}_{i\theta}$ and $l^{(2)}_{i\theta}$, realize a *soft*-gating mechanism: V1 activities which are selectively enhanced by matching V2 contour cell activation in turn provide more inhibitory energy in the normalization stage. Thus, salient contrast arrangements will be enhanced while at the same time spurious and perceptually irrelevant responses will we suppressed by way of inhibition. In Appendix 1 we present details of this soft-gating mechanism.

Model V2. Arrangements of graded contrast activities are fed forward to orientation selective

contour cells in area V2. Local contrasts appear as part of smooth continuous shape contour outlines. Therefore, a significant response measured by localized contrast cells is frequently part of a curvilinear arrangement of co-occurring contrast cell responses. The presence of coherent outlines with different curvature is encoded in a weighting pattern of connectivity that preferentially links cells of smooth contours in space/orientation domain which tangentially pass through the target location. An oriented RF weighting function of a contour cell is thus considered as 'contour template' (compare Mumford, 1994) to match the likely presence of smooth shape outlines. Using this mechanism, in the first stage of model V2 the significance of a target cell response for a given orientation is evaluated on the basis of the accumulation of weighted input in the spatial neighborhood. In order to reduce the uncertainty of measurement along its axis of elongation we partition the 'contour template' into several components. Each component contributes to the final matching activity of the V2 target cell. We use a bipartite RF that consists of two separate lobes which sample opposite half-planes along their symmetry-axis (see Fig. 2, left). A non-linear accumulation stage subsequently integrates the activities from a colinear pair of lobes (Grossberg and Mingolla, 1985; Peterhans and von der Heydt, 1989) which requires input activation from *both* branches. Functionally, such a mechanism implements an AND-gate of activities from opposite half-planes such that a contour cell only gets activated if it signals a continuous contour segment. This is consistent with physiological findings about non-linearities in the response of V2 contrast cells (e.g. von der Heydt *et al.*, 1984; see Section 2).

The weighting functions of both branches consist of ON- and OFF-subfield components (Fig. 2, right) denoted by $\Gamma^{\pm,L}_{i\theta}$ and $\Gamma^{\pm,R}_{i\theta}$, respectively. ON-subfields display the pattern of excitatory weightings in space/orientation for localized contrast cells to facilitate the V2 target cell. Fig. 2 (right, top) shows a target cell that is tuned to horizontal orientation. An additional inhibitory weighting pattern is defined by the OFF-subfield. This incorporates the non-relatability constraint (Kellman and Shipley, 1991) and makes the integration in space/orientation domain more selective and tuned to significant contrast arrangements. We investigated different patterns of inhibitory weighting, including maximal suppression for orientations orthogonal to the supportive contrast orientations. The simplest scheme of coarse iso-orientation inhibition turned out to be most effective concerning a broad range of stimulus configurations (Fig. 2, right, bottom). Appendix 2 contains a description of the scheme to create the weighting functions. Input activation from both branches of a 'contour template' at position i for orientation θ is computed by the convolutions $l^{(2)}\star\Gamma^{\pm,L}_{i\theta}$ and $l^{(2)}\star\Gamma^{\pm,R}_{i\theta}$. Since contributions of excitatory and inhibitory weightings enter in an additive fashion, we get $v^{L}_{i\theta} = \max[\{l^{(2)}\star(\Gamma^{+,L} - \Gamma^{-,L})\}_{i\theta}, 0]$ and $v^{R}_{i\theta} = \max[\{l^{(2)}\star(\Gamma^{+,R} - \Gamma^{-,R})\}_{i\theta}, 0]$. Incorporating a rectification operation prevents incompatible contrast configurations from generating

dominant negative responses via OFF-subfield integration.

Our V2 RF model is based on the bipole concept of long-range interaction first suggested by Grossberg and Mingolla (1985). However, unlike their approach we utilize a micro-circuit that realizes the functionality of an AND-gate via a mechanism of self-inhibition and disinhibition. In addition to the computation of $v_{i\theta}^L$ and $v_{i\theta}^R$ activities, two additional network stages establish the AND-gate functionality generating $h_{i\theta}^{(1)}$-responses (Fig. 2, center). Consider the case in which only one branch, say the left one, receives activation. Along the left branch, initial $v_{i\theta}^L$ activity excites the $r_{i\theta}^L$ cell which is inhibited by $q_{i\theta}^L$. Since the opposite branch has zero-level activation, self-inhibition of $v_{i\theta}^L$-activity leaves the target cell unexcited. Now consider the case that *both* branches receive significant activation. As in the first case, initial activation from left *and* right branches generate excitations $r_{i\theta}^L$ and $r_{i\theta}^R$ that are self-inhibited via $q_{i\theta}^L$ and $q_{i\theta}^R$ activation, respectively. In addition, now cross-inhibition of self-inhibitory nodes generate a disinhibition of activity for each branch. Only now the node at the final stage can get activated to generate a $h_{i\theta}^{(1)}$-response. In all, the mechanisms of self-inhibition of individual lobes and disinhibition of activation among subfield branches guarantee that the target cell generates a response *only* when both branches get activated simultaneously.

The different stages of the micro-circuit generate activities on the basis of steady-state shunting interactions. The net effect of a lumped representation of $h_{i\theta}^{(1)}$ cell response results in a multiplicative, or gating-like, combination of activity from both branches, $v_{i\theta}^L$ and $v_{i\theta}^R$. Formally, we get the equilibrium activity

$$h_{i\theta}^{(1)} = v_{i\theta}^L v_{i\theta}^R \frac{\frac{2}{\zeta_3} + v_{i\theta}^L + v_{i\theta}^R}{\frac{1}{\zeta_3^2} + \frac{1}{\zeta_3}\left(v_{i\theta}^L + v_{i\theta}^R\right) + v_{i\theta}^L v_{i\theta}^R}. \tag{3}$$

In Appendix 3 we present the individual stages of the micro-circuit that generate the final response in Eqn. 3. Parameter ζ_3 determines the shape of compressive non-linear function that transforms the input activation and therefore determines the responsiveness to graded V1 input. In the limit $\zeta_3 \to \infty$, the contour response is defined by the sum of input from both bipole branches. In all, contour cells are devices which selectively respond only for cocircularly aligned contrast arrangements measured at *both* sides of a target location. In addition, we investigated the activation in response to imbalanced input arrangements. For constant *average* input, $\bar{v}_{i\theta}$, the contour cell encodes any imbalance in the input through a monotonic reduction of responsiveness. The shape of the response function is defined by

$$h_{i\theta}^{(1)}(k) = 2\bar{v}_{i\theta} - \frac{1}{\zeta_3}\frac{1+2k^2}{1-k^2}, \tag{4}$$

where $k \in [0, 1)$ denotes the deviation of input activity from a given average level. Thus, the cell is selective to the structural coherence of the input such that any imbalance of input from both branches reduces the response amplitude in a monotonic fashion. In Appendix 3 we present details of this investigation.

Similar to V1, $h_{i\theta}^{(1)}$-activities from the the previous matching stage undergo a center-surround competition between activations in a local spatial neighborhood over orientations to generate the new activation $h_{i\theta}^{(2)}$. A shunting mechanism realizes a saturation-type normalization by divisive inhibition. Again we assume fast relaxation to equilibrium response such that we use the resulting steady-state response of the local first-order interaction

$$h_{i\theta}^{(2)} = \frac{\beta_4 h_{i\theta}^{(1)} - \delta_4 \left\{ h_{i\theta}^{(1)} \star \Psi^- \star \Lambda^- \right\}_{i\theta}}{\alpha_4 + \zeta_4 \left\{ h_{i\theta}^{(1)} \star \Psi^- \star \Lambda^- \right\}_{i\theta}}, \tag{5}$$

where α_4, β_4, δ_4, and ζ_4 are constants. The $h_{i\theta}^{(2)}$-activations are subsequently fed back via the descending pathway to enhance the activities of initial measurements from V1 oriented contrast cells (see Eqn. 1).

4 Computational Experiments and Simulation Results

The network architecture has been implemented and tested on a variety of stimuli. All linear equations for local feedforward interaction have been solved at equilibrium. The non-linear Eqn. 1 was solved numerically using a 4th-order Runge Kutta scheme with adaptive step size control (Press *et al.*, 1989). We subsequently compared the final arrangement of responses with those acquired by an approximate scheme using fix-point iteration of equilibrated responses of Eqn. 1. Yet there were no observable differences in results after four iterations of the recurrent network. Therefore, in order to reduce computing time, we have used the approximate scheme to generate the set of simulation results shown below. In Appendix 4 we summarize the equations and provide all parameter settings.

We conducted a series of computational experiments with the primary goal demonstrating the role of recurrent interaction. Specifically, we show the influence of a broader context represented by V2 contour cell activations to modulate more localized measurements at the earlier stage in V1. We investigated several phenomena summarized in Section 2 in order to demonstrate the explanatory capacity of the proposed model. In particular, we present results for integrating and interpolating input patterns via the V1–V2 feedforward stream, the tuning of selectivity of V1 cells via feedback processing, the induction of context effects via facilitory and inhibitory feedback

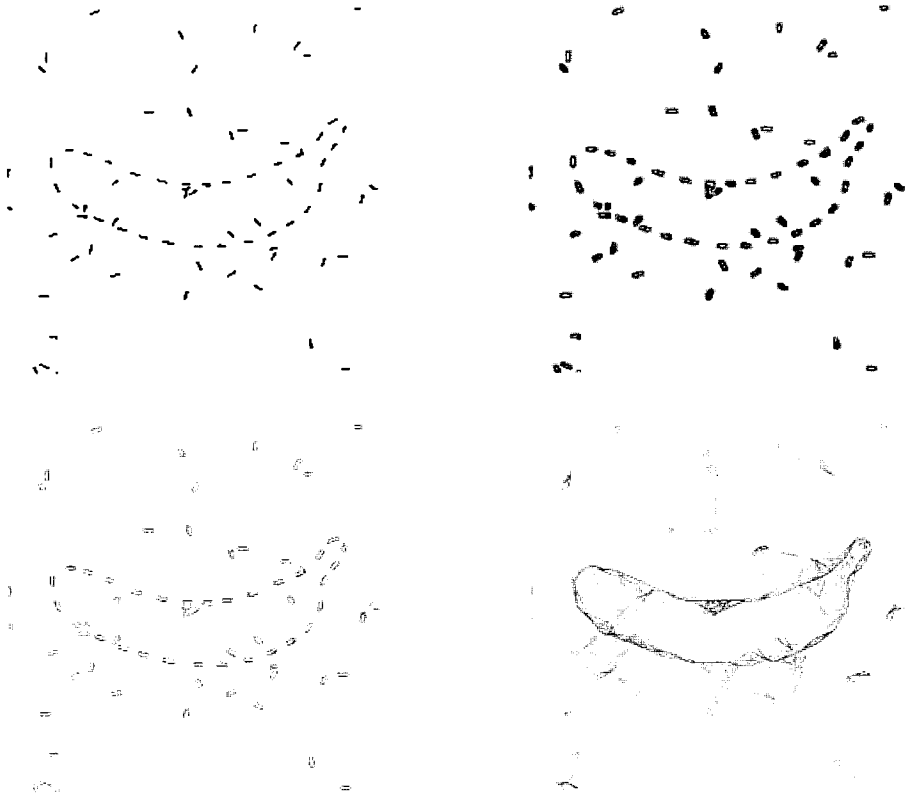

Figure 3: *Processing of a noisy fragmented shape outline. Top left: Input image; Top right: Responses of contrast detection stage utilizing oriented filters (simple cells), c; Bottom left: Equilibrated normalized model V1 cell responses,* $l^{(2)}$*; Bottom right: Equilibrated model V2 cell responses utilizing 'contour templates',* $h^{(2)}$*. Responses saturate after four cycles of iteration.*

interaction, as well as the generation of illusory contour responses via cortico-cortical recurrency.

Consider a stimulus of noisy fragmented shape outline (Fig. 3, top, left). V1 simple cells respond to individual bars generating a distribution of local contrast activation (Fig. 3, top, right). The subsequent stage of contrast enhancement and normalization slightly reduces the space/orientation uncertainty but still leaves a fuzzy representation of bar items. These activities are fed forward to V2 cells which match 'contour templates' against the arrangement of initial responses. Those items which are part of coherent curvilinear shape outlines generate high contour activation whereas more isolated items produce only minor activation. By way of long-range integration using bipolar weighting functions the fragmented shape is interpolated to generate a continuous representation of shape in V2. In addition, other configurations also generate candidate groupings although represented by weaker responses compared to the central figure (Fig. 3, bottom, right). We suggest that the contrast enhanced and normalized V2 activity distribution represents an adaptive code pattern (Grossberg, 1980; Mumford, 1994) that is used to modulate the inital contrast measure-

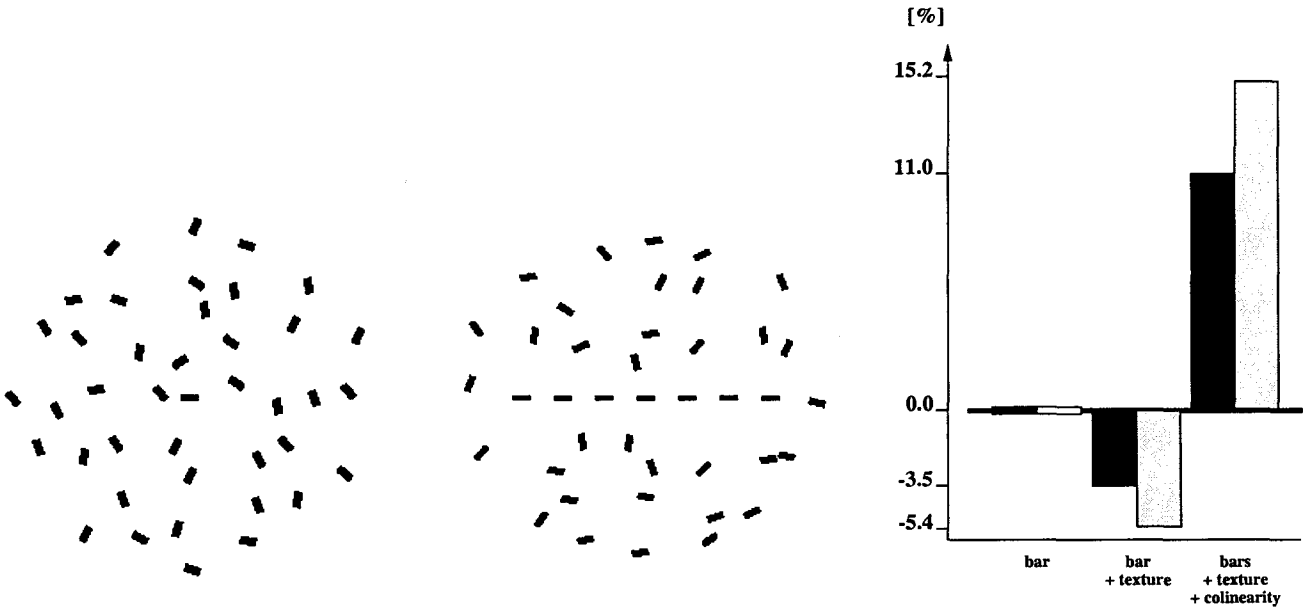

Figure 4: *Processing results for a texture stimulus composed of oriented bars. Left: Stimulus pattern with a central bar embedded in a texture with randomly oriented bar items; Center: Texture stimulus in which the central bar item is supported by aligned bars of the same orientation; Right: Equilibrated model V1 cell responses* $l^{(1)}$ *for the central bar as a function of the top-down gain control parameter C (see Eqn. 1) for different stimuli. Percent change in activation is shown relative to the activity in response to an isolated bar. Shaded bars display results for different values of the gain control factor C (black:* $C = 5$*, grey:* $C = 10$*; see text for discussion).*

ments at V1. In other words, the activities of an interpolated ‚shape selectively enhance initial V1 activations via an increased gain from retinotopic feedback connections. The result of recurrent feedforward/feedback processing is a distribution of sharply localized V1 contrast responses (Fig. 3, bottom, left) which in turn also help sharpen the interpolated contour groupings in V2. The model predictions are consistent with a number of physiological and psychophysical findings. The alignment of multiple bars outside a V1 cell RF increases the response at the target location (Kapadia *et al.*, 1995). This facilitation is consistent with perceptual effects of contour detection in texture patterns (Field *et al.*, 1993). V2 contour cells respond to fragmented outlines generated by grating bars and illusory bars (Peterhans and von der Heydt, 1989, 1993). A facilitation of threshold contrast detection of the same amount has been observed for line gaps as well as illusory contours (Rieger and Gegenfurtner, 1998). Moreover, the effects were independent of whole figural presentation, which suggests a contour oriented mechanism.

The magnitude of facilitation by the top-down gain control mechanism was investigated in more detail using texture stimuli of the type used by Kapadia *et al.* (1995). We claim that the feedback of contour code patterns generates 'extra-RF modulation' of V1 responses (Zipser *et al.*, 1996) that

contributes to the surround inhibition in textures (Knierim and VanEssen, 1992; Kapadia *et al.*, 1995). An individual bar has been processed to get responses that are used as a reference. The same bar was then embedded in a texture of randomly orientated bars. Subsequently, the central bar was supplied by a row of aligned same orientation bars (Fig. 4, left and center). Stimulus processing in model V1 again generates a representation of sharply localized contrast responses for individual bar items. Model V2 contour cells generate local candidate groupings of low activation for random orientations. As a result, only minor feedback is generated for the central bar. In the stimulus with aligned bars which are supplied colinearly salient grouping is generated and a higher-order unit is formed by V2 contour processing. The resulting feedback activity selectively enhances the bar at the center of the texture. Figure 4 (right) confirms the prediction by showing the percent change in activation in comparison to the isolated bar. In order to demonstrate the role of the feedback gain constant C, we show results for two different magnitudes. The values have been chosen to lie within the bounds derived in Appendix 1. The results are consistent with the results of Knierim and VanEssen (1992) and Kapadia *et al.* (1995), showing a reduction of response when the bar is part of a random texture. Strong enhancement occurs when the central bar in the texture is part of a salient arrangement of colinear bars. In addition, we demonstrate the influence of the constant C in Eqn. 1 on the results. Interestingly, an increase in the gain not only increases the facilitation in the supplement case but also increases the suppression effect for the random texture. In the model the latter is a consequence of the stronger surround inhibition that develops in the course of several iterations at the stages of normalizing V1 and V2 cell responses, respectively.

Experiments by Baumgartner and coworkers (Baumgartner *et al.*, 1984; von der Heydt and Peterhans, 1989) have demonstrated that V2 contour cells respond to occluding contours generated by oriented abutting gratings (Fig. 5, top left). Our network simulations demonstrate that V1 cells signal the boundaries of individual bars whereas at V2 contour cells also generate sharply localized interpolations between line endings, thus generating illusory contours (Fig. 5, top center & right). The strength of illusory contours depends on the number and density of lines in the integration field. This is in accordance with the studies of Baumgartner *et al.* (1984) (see also Peterhans and von der Heydt, 1991). Our focus of investigation again is the top-down modulation of V1 measurements. We investigated the response of cells tuned to different orientations at a line ending in the center of the stimulus. Initially, responses for different orientations were rather unspecific. Thus, each individual cell shows a broad orientation tuning (compare Ringach *et al.*, 1997). Now, the significant grouping of cell responses at V2 for the horizontal orientation kicks in and in turn, by way of feedback gain control, selectively enhances V1 cells for the corresponding orientation ($\theta = 0$

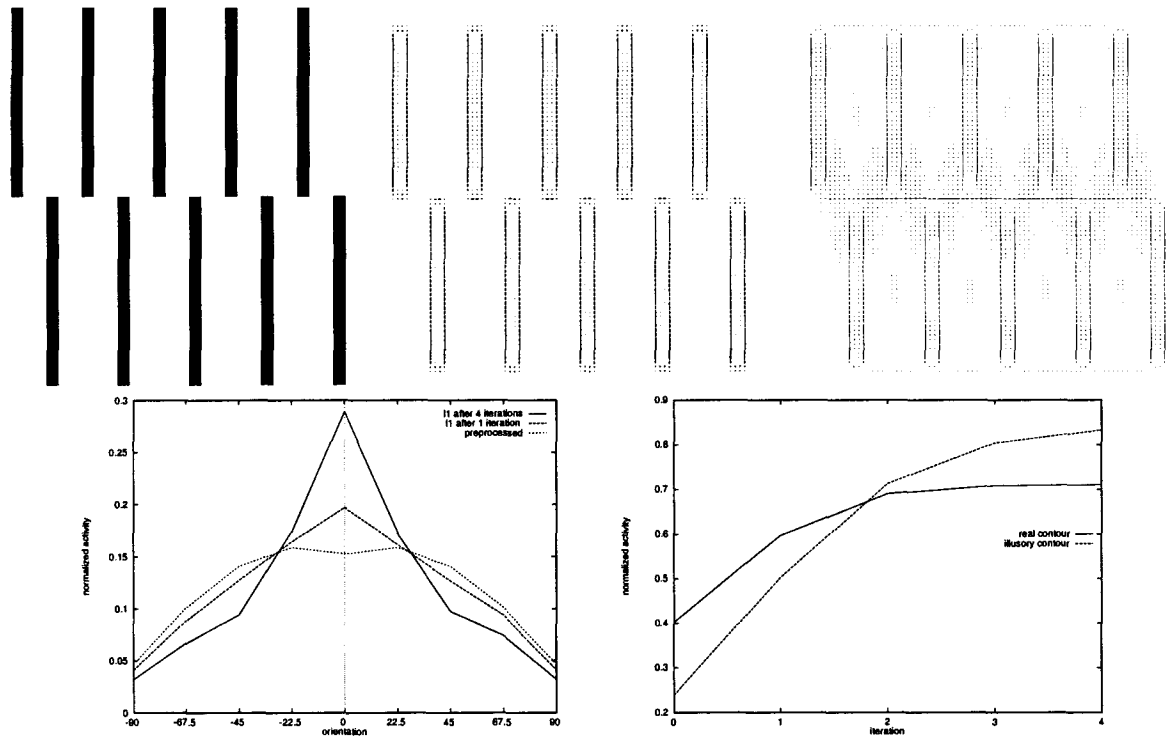

Figure 5: *Processing an abutting grating pattern composed of oriented bars. Top, left: Input pattern. Top, center: Equilibrated model V1 cell responses $l^{(2)}$ that highlight the boundaries of the individual bars. Top, right: Equilibrated model V2 cell responses $h^{(2)}$ for the grating pattern. Cell activities are generated for horizontal illusory contour locations with high activation level at the center and with less activation at the top and bottom lines (compare [von der Heydt and Peterhans, 1989]). Bottom, left: Initial processing at line ends shows an unspecific $l^{(1)}$ response corresponding to a broad orientation tuning. Recurrent interaction signals a perceptually significant horizontal (illusory) contour. In the course of temporal evolution over four cycles of iteration the activity saturates with a reduced orientational uncertainty building up a dominant selectivity to horizontal orientation. Bottom, right: Temporal development of V2 cell responses $h^{(2)}$ for a contour at real contrasts and an illusory contour (see text for discussion).*

in Fig. 5, bottom, left). V1 cell responses saturate after four cycles of iteration. Along this time course, we observe that responses for the horizontal orientation are significantly increased whereas at the same time responses for the other orientations are reduced. The findings are consistent with those investigating the change in orientation selectivity of V1 cells by flanking bars (Gilbert and Wiesel, 1990). In all, the tuning curves of the target cells were shifted by the inhibition of flanking items. Using our model such an effect can be explained as a combination of increased gain for a different dominant orientation which in turn increases the inhibition for a target cell. Our model predicts that compared to a physical contrast the illusory contour strength for the grating develops more gradually over time. Initially, since the V1 cells respond rather unspecific, also

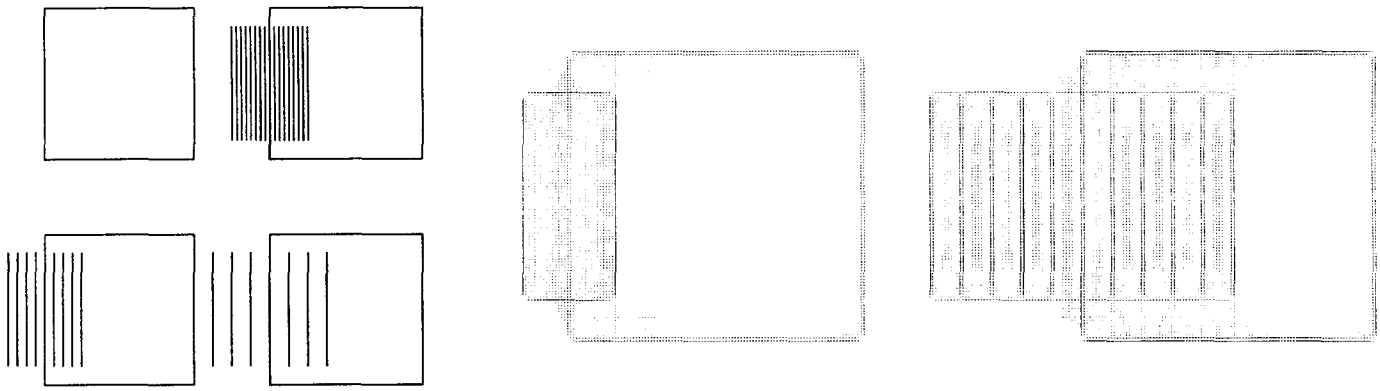

Figure 6: *Demonstration of different contour responses which depend on the local context and density of contour arrangement. Left: Input stimulus with a plain square line arrangement and three versions of the same square overlayed with texture regions of varying line densities; Center:* $h^{(2)}$*-responses of model V2 cells for the square line pattern with a dense bar texture which appears as a coherent surface region in front of the square; Right:* $h^{(2)}$*-responses of model V2 cells for the same square line pattern overlayed by a texture of wide bar separation – the region has lost its structural coherence against the square and thus the apparent occlusion and figure-ground segregation disappears.*

the interpolated contour should be shallow. As the V1 cell selectivity is sharpened by consistent top-down enhancement, V2 contour cells generate localized reponses of high amplitude. Figure 5 (bottom, right) shows this result for two selected model V2 cells. A luminance contrast is registered already in the first pass of bottom-up processing. The initial response is further enhanced to generate a saturated activity for the contour of a vertical bar. For the horizontal illusory contour in the center the response develops more gradual. In the beginning a minor response is present (see the discussion in von der Heydt and Peterhans, 1989). This response increased over time until saturation as the responses for the horizontal orientation are progressively enhanced via feedback interaction. The saturated illusory contour response is even higher than for the luminance contrast. This is consistent with the results shown by Baumgartner *et al.* (1984) (see also von der Heydt *et al.*, 1984) indicating a better cell response to the illusory contour of an abutted grating than to a bar. We observe an increasing strength of response as a function of the number of inducing line ends. This is consistent with the data shown by von der Heydt *et al.* (1984). In its limit, an arrangement of one-sided line endings merges to generate a continuous luminance contrast. The simulations results in Fig. 5 (bottom, right) thus predict that the response amplitude is reduced for increased density of bars due to stronger inhibition generated by the feedback as well as the competitive interactions at the stage of V1 interaction. This, in turn, is consistent with the inverted U-shaped function of perceptual contour strength measured by Lesher and Mingolla (1993) for Varin figures with varying line density.

A final experiment investigates the dependency of contour perception on spatial configuration effects. Figure 6 (left) shows four squares. If a border line is surrounded by bar segments of the same thickness, the individual line of the square boundary gets lost, depending on the density of the flanking bars (compare with Kanizsa, 1968). As suggested by Mumford (1994) a perceptual system should generate a representation that is in accordance with the spatial context. Thus, individual responses based on local measurements might appear different in varying contexts of visual stimulation. Figure 6 (center & right) demonstrates this for the dense arrangement as well as the wider separated flanking bars. In the first case, V2 contour cells generate a rectangular shape outline for the texture. Top and bottom endings are interpolated generating an illusory contour. The line that belongs to the square is almost absorbed by a significant reduction in contour response. If the texture bars were increasingly more separated spatially, responses were generated for individual lines. The central square line appears at the same strength as the other bars. Their perceptual belonging is represented by the interpolation between their aligned top and bottom line endings. We suggest that the mechanisms of our model therefore play an important role in surface segmentation and shape recognition.

5 Summary and Discussion

In this paper, we first propose a computational framework for bidirectional visual cortical processing, namely of recurrent V1 and V2 interaction, that helps linking physiology and psychophysics. Second, we present a model of modulation of initial V1 responses by context dependent top-down V2 contour cell activation. In general, for a pair of cortical areas the "lower area" is considered as a stage of signal measurement whereas the "higher area" evaluates the significance of arrangements of local activity patterns based on context information. The results of simulations unify several seemingly unrelated experimental findings. This suggests a novel interpretation of the role of contour interpolation at V2 such that observable effects relate to the task of surface segmentation and that this information is used to evaluate and guide initial measurements at earlier stages of processing. Thus, the model links physiological and perceptual findings. Results of processing several test stimuli predict texture density effects, excitatory as well as inhibitory top-down influences and effects of temporal development of sharpness and amplitude of perceptual contours. Finally, we propose a unified scheme for contour integration using 'contour templates' that incorporate selective subfield integration, spatial relatability constraints and cocircularity measurements.

Our work is related to several other models. Other approaches have been proposed that utilize recurrent processing for contour extraction. For example, Grossberg and Mingolla (1985) proposed

the Boundary Contour System (BCS) which consists of a stage of oriented contrast detection and a recurrent competitive-cooperative loop for long-range contour integration. A slightly revised version of the original BCS serves as basic modular building block for a model of recurrent intracortical contour processing at V1 and V2 (Grossberg *et al.*, 1997). The modular design of cortical circuits follows the suggestion that V1 and V2 circuitry is spatially homologous utilizing a more broadly tuned spatial scale at the higher cortical area. Oriented lateral interactions of different spatial ranges using bipole weighting functions are suggested to implement the function of horizontal connections between oriented cells in V1 and V2 layers 2/3 (Gilbert, 1992; Malach *et al.*, 1994). Our model differs from the extended BCS in several ways. The key aspect of the development is the recurrent interaction *between* cortical areas V1 and V2. The claim is that activity integrated from separate sites at the "higher" area (model V2) is used to assess the activity distribution in the "lower" area (model V1). Thus, we suggest an instantiation of how *cortico-cortical* feedback interaction might work to evaluate initial measurements in terms of a broader visual context. Unlike the BCS, in our model contour interpolation is mainly feedforward driven without any inward spreading process that completes (or fills-in) activities between inducers. Spatially segregated inducers are integrated along the bottom-up stream by space/orientation filtering using elongated bipole 'contour templates'. The compatibility measure that is encoded in the connectivity pattern of these weighting functions utilizes a similar support function as proposed by Parent and Zucker (1989). In order to enhance the selectivity of the support function, these authors incorporated a binary predicate to evaluate the consistency of symbolic curvature classes for candidate groupings between tangents. In our scheme, the excitatory field of cocircular tangent orientations is supplied by a field of inhibitory weightings to penalize non-relatable pairs of contrast orientation (Kellman and Shipley, 1991). Furthermore, we do not include any explicit symbolic labeling of activities according to a discrete set of curvature classes. Activities that might belong to conflicting interpolations compete such that most prominent arrangements will provide strongest top-down gain. In turn, those activities compatible with such a dominant grouping will further sharpen the representation of spatially interpolated contour segments.

Similar to the BCS bipole cell functionality, but unlike Zucker's scheme, the input from different branches is integrated in a non-linear way to resemble an AND-gate functionality. The interpolation in a feedforward process is in accordance with the model proposed by Heitger *et al.* (1998). However, this model and a previous version proposed by von der Heydt and Peterhans (1991) builds upon selective integration of end-stop responses that are generated at corners and line terminations. This grouping stage is kept separate from processing of physical luminance contrasts. The output of the distinct activity distributions are subsequently integrated to build a final contour

representation. Such a selective integration of line terminators has also been used in the model of Finkel and coworkers (Finkel and Edelman, 1989; Finkel and Sajda, 1992) to explicitly signal the presence of surface occlusions. Unlike Heitger's scheme, we do not utilize any segregated processing streams which selectively integrate responses from end-stop neurons. Instead, activities from initial contrast measurement are sharpened by way of feedback modulation – an option that has been abandoned in the models of Heitger, von der Heydt and colleagues. The result of spatial integration of contrast signals is supposed to serve as a reference, or 'expectation', to assess the significance of individual input measurements.

Zucker (1985) proposed a probabilistic relaxation scheme for iterative updating normalized contrast activities in different orientations. Each measure of locally oriented contrast is evaluated on the basis of the spatial support from contrast activations in a local neighborhood. We have instead segregated the assessment of contrast activations via a gain control mechanism and the contour interpolation into separate stages. In accordance to recent empirical data our model generates representations of visual surface contours including (illusory) contour interpolations and the context dependent modulation of local activity measurements. Li (1998a,b) recently proposed a model of cortical contour integration. This model also utilizes oriented weighting functions for compatibility measurement in texture boundary detection. As already pointed out by Li, her model is similar to the V1 stage of processing of Grossberg *et al.* (1997). It should be noted that we do not deny the existence of oriented horizontal long range connections at the stage of V1 processing. In fact, in the model outlined here, we wanted to focus exclusively on the issues of top-down interaction. Therefore, we excluded any additional components that might interfere with the functionality of the recurrency. Our investigation is thus complementary to these investigations as it provides the so far excluded input from extra-striate processing as suggested in our model.

Other approaches have focussed on the integration of multiple visual cues to generate coherent percepts. For example, Edelman and coworkers have presented large scale simulations of the integration of coarse grain visual representations between segregated visual areas. Finkel and Edelman (1989) combine motion and contour processing for the generation of coherent surface percepts, whereas Tononi *et al.* (1992) focussed on the interaction between multiple cortical areas utilizing a lumped V1/V2 model on an even more abstract level of description. Unlike our approach, their computational strategies for dynamic conflict resolution are guided by explicit occlusion properties and associated illusory contour generation. This approach was further pursued by Finkel and Sajda (1992) proposing to link together contrasts and surfaces in order to define object related groupings instead of "thingless" units. We appreciate the influence of processing from even higher cortical stages, such as MT, V4 and IT, on early V1 processing of surface related

information. However, we have focussed our investigation on the more detailed mechanisms of *contour* processing among V1 and V2. Our investigation demonstrates how the dynamics of such a scheme of recurrent interaction may resolve ambiguities without the need of extra instances to handle occlusion or top-down reentrance conflicts.

Our architecture integrates concepts of the more general computational frameworks described by Mumford (1991, 1994) and Ullman (1995). Inspired by basic principles of pattern recognition, the descending pathways in recurrent loops between cortical areas are suggested to carry flexible templates which are compared with the properties of the sensory input (Mumford, 1991). A central element of this proposal is that the measure of fit between signal data and a flexible template is represented by their difference. Mumford suggested that the bottom-up pathway should carry this residual activity pattern. Rao and Ballard (1997) incorporated these concepts into a hierarchical predictor for data processing formulated in the framework of control and stochastic prediction theory. In their approach, input stimuli are processed through a hierarchical sequence of filtering stages. The output of the associated feedforward projection determines the state of the network at the subsequent model area. Given the bottom-up filtered signal data, a prediction of the expected state of the previous area is generated via a set of top-down filters. The difference between the actual activity distribution (that determines the state) and the predicted one results in a residual that is in turn filtered and fed forward again. The authors successfully demonstrated the capability of the network in object recognition tasks. They also show how end-inhibition in V1 cells might be generated by the influence of top-down feedback (Rao and Ballard, 1996). It should be noted, that many of these principles are similar to the computational mechanisms in ART-networks for input registration and stable category learning (Carpenter and Grossberg (1988); see Grossberg (1980) for the general computational principles). Unlike the proposal of processing residuals, mismatches are detected which subsequently trigger a reset signal to switch off activated category nodes which represent any object instances. In our model, top-down activation is rather low-level and triggered by the current stimulus configuration. Therefore, any mismatch between input activation and top-down code pattern is signalled more indirectly by a reduction in modulation strength and subsequent reduction in activity via local competitive processes. Thus, local signal measurements that do not fit the broader arrangement of contour shape are weakened or even suppressed.

The weighting pattern of our V2 contour templates is designed to support smooth contours of varying curvature. These templates are flexible in that they carry segments of frequently occurring shapes including their variance in terms of local curvature (Mumford, 1994). Ullman (1995) puts emphasis on necessary testing of multiple alternatives of object hypotheses to be matched against the signal data utilizing counter-streams of bottom-up and top-down processing. We suggest that

in the case of recurrent V1–V2 interaction the ascending pathway carries an input representation of the stimulus. The 'contour templates' representing a range of curvatures are matched for different orientations. The result is a field of activities whose relative magnitudes are proportional to the degree of matching strength derived by the contour interpolation. These candidate groupings are fed back in parallel along the descending pathway to selectively control the gain for enhancing the initial activations. Thus, we suggest that the simultaneous testing of possible alternatives (Ullman, 1995; Mumford, 1994) is realized by the gain-control mechanism and subsequent center-surround competition in the space/orientation domain.

In all, we suggest a computational framework of how the feedback pathways might be used to assess localized measurements in previous stages of the cortical hierarchy. We particularly focussed on the recurrent processing of contour information in cortical areas of V1 and V2. In this paper we do not attempt to develop a model that generates biologically realistic responses. Instead, the different stages represent abstractions of functionality with the goal of describing the basic computational principles of recurrent contour processing. The general principles proposed in our model are not limited to the early stage of V1 and V2. We claim that we can extend our modeling for motion as well as shape processing utilizing recurrencies between areas V1/V2 and MT and V4 and IT, respectively.

Acknowledgements. We are grateful to Alexander Grunewald and Thomas Wennekers for insightful comments that further enhanced the manuscript.

References

Barrow, H.G. and Tenenbaum, J.M. (1981). Interpreting line drawings as three-dimensional surfaces. *Artif. Intell.*, **17**, 75-116.

Baumgartner, G., von der Heydt, R., and Peterhans, E. (1984). Anomalous contours: A tool in studying the neurophysiology of vision. *Exp. Brain Res. (Suppl.)*, **9**, 413-419.

Beck, J., Rosenfeld, A., and Ivry, R. (1989). Line segregation. *Spatial Vis.*, **4**, 75-101.

Bullier, J., McCourt, M., and Henry, G. (1988). Physiological studies on the feedback connection to the striate cortex from cortical areas 18 and 19 of the cat. *Exp. Brain Res.*, **70**, 90-98.

Carpenter, G.A. and Grossberg, S. (1988). The ART of adaptive pattern recognition by a self-organizing neural network. *Computer*, **21**, 77-88.

Crick, F. (1984). Function of the thalamic reticular complex: The searchlight hypothesis. *Natl. Acad. of Science USA*, **81**, 4586-4590.

DeAngelis, G.C., Ohzawa, I., and Freeman, R.D. (1993). Spatiotemporal organization of simple-cell receptive fields in the cat's striate cortex. II. Linearity of temporal and spatial summation. *J. Neurophys.*, **69**, 1118-1135.

DeYoe, E. and Van Essen, D. (1988). Concurrent processing streams in monkey visual cortex. *Trends in Neurosci.*, **11**, 219-226.

Eckhorn, R., Reitboeck, H.J., Arndt, M., and Dicke, P. (1990). Feature linking via synchronization among distributed assemblies: Simulations of results from cat visual cortex. *Neural Comp.*, **2**, 293-307.

Field, D.J., Hayes, A., and Hess, R.F. (1993). Contour integration by the human visual system: Evidence for a local "association field". *Vis. Res.*, **33**, 173-193.

Finkel, L. and Edelman, G.M. (1989). Integration of distributed cortical systems by reentry: A computer simulation of interactive functionally segregated visual areas. *J. Neurosci.*, **9**, 3188-3208.

Finkel, L. and Sajda, P. (1992). Object discrimination based on depth-from-occlusion. *Neural Comp.*, **4**, 901-921.

Gilbert, C. (1992). Horizontal integration and cortical dynamics. *Neuron*, **9**, 1-13.

Gilbert, C. and Wiesel, T.N. (1989). Columnar specificity of intrinsic horizontal and corticocortical connections in cat visual cortex. *J. Neurosci.*, **9**, 2432-2442.

Gilbert, C. and Wiesel, T.N. (1990). The influence of contextual stimuli on the orientation selectivity of cells in primary visual cortex of the cat. *Vis. Res.*, **30**, 1689-1701.

Gilchrist, I.D., Humphreys, G.W., Riddoch, M.J., and Neumann, H. (1997). Luminance and edge information in grouping: A study using visual search. *J. Exp. Psych.: Human Perc. Perform.*, **23**, 464-480.

Ginsburg, A.P. (1987). The relationship between spatial filtering and subjective contours. In S. Petry and G.E. Meyer (eds.) *The perception of illusory contours*, New York, Springer.

Glass, L. (1969). Moiré effect from random dots. *Nature*, **223**, 578-580.

Glass, L. and Pérez, R. (1973). Perception of random dot interference patterns. *Nature*, **246**, 360-362.

Grossberg, S. (1980). How does a brain build a cognitive code? *Psychol. Rev.*, **87**, 1-51.

Grossberg, S. and Mingolla, E. (1985). Neural dynamics of perceptual grouping: Textures, boundaries, and emergent segmentation. *Perc. and Psychophys.*, **38**, 141-171.

Grossberg, S., Mingolla, E., and Ross, W.D. (1997). Visual brain and visual perception: How does the cortex do perceptual grouping? *Trends in Neurosci.*, **20**, 106-111.

Heeger, D.J. (1992). Normalization of cell responses in cat striate cortex. *Vis. Neurosci.*, **9**, 184-197.

Heeger, D.J., Simonchelli, E.P., and Movshon, J.A. (1996). Computational models of cortical visual processing. *Proc. Natl. Acad. Sci.*, **93**, 623-627.

Heitger, F., von der Heydt, R., Peterhans, E., Rosenthaler, L., and Kübler, O. (1998). Simulation of neural contour mechanisms: Representing anomalous contours. *Image and Vis. Comp.*, **16**, 407-421.

Hubel, D.H. and Wiesel, T.N. (1968). Receptive fields and functional architecture of monkey striate cortex. *J. Physiol.*, **195**, 215-243.

Kanizsa, G. (1968). Percezione attuale, esperienza passata è l'"esperimento impossibile". In G. Kanizsa and G. Vicario (eds.) *Ricerche sperimentali sulla percezione*, Triente, Università degli studi.

Kanizsa, G. (1976). Subjective contours. *Sci. Am.*, **234**, 48-52.

Kapadia, M.M., Ito, M., Gilbert, C.D., and Westheimer, G. (1995). Improvement in visual sensitivity by changes in local context: Parallel studies in human observers and in V1 of alert monkeys. *Neuron*, **15**, 843-856.

Kastner, S., Nothdurfth, H.-C., and Pigarev, I. (1996). The spatial extent of contextual response modulations in cat striate cortex. *Soc. Neurosci. Abstr.*, **22**, 284 (#117.11).

Kellman, P.J. and Loukides, M.G. (1987). An object perception approach to static and kinetic subjective contours. In S. Petry and G.E. Meyer (eds.) *The perception of illusory contours*, New York, Springer.

Kellman, P.J. and Shipley, T.F. (1991). A theory of visual interpolation in object perception. *Cogn. Psychol.*, **23**, 141-221.

Knierim, J.J. and Van Essen, D.C. (1992). Neuronal responses to static texture patterns in area V1 of the alert macaque monkey. *J. Neurophys.*, **67**, 961-980.

Krubitzer, L.A. and Kaas, J.H. (1989). Cortical integraton of parallel pathways in the visual system of primates. *Brain Res.*, **478**, 161-165.

Lamme, V.A.F. (1995). The neurophysiology of figure-ground segregation in primary visual cortex. *J. Neurosci.*, **15**, 1605-1615.

Lamme, V.A.F., Zipser, K., and Spekreijse, H. (1997). Figure-ground signals in V1 depend on extrastriate feedback. *Inv. Ophthal. Vis. Science*, **38**(4), S969 (PGM #4490).

Lesher, G.W. (1995). Illusory contours: Toward a neurally based perceptual theory. *Psychon. Bull. and Rev.*, **2**, 279-321.

Lesher, G.W. and Mingolla, E. (1993). The role of edges and line-ends in illusory contour formation. *Vis. Res.*, **33**, 2253-2270.

Li, Z. (1998a). A neural model of contour integration in the primary visual cortex. *Neural Comp.*, **10**, 903-940.

Li, Z. (1998b). Pre-attentive segmentation in the primary visual cortex. MIT, AI Lab, AI Memo No. 1640.

Livingstone, M. and Hubel, D. (1984). Anatomy and physiology of a color systems in the primate visual cortex. *J. Neurosci.*, **4**, 309-356.

Malach, R., Tootell, R., and Malonek, D. (1994). Relationship between orientation domains, cytochrome oxidase stripes and intrinsic horizontal connections in squirrel monkey area V2. *Cerebral Cortex*, **4**, 151-165.

Mumford, D. (1991). On the computational architecture of the neocortex II: The role of cortico-cortical loop. *Biol. Cybern.*, **65**, 241-251.

Mumford, D. (1994). Neuronal architectures for pattern-theoretic problems. In C. Koch and J.L. Davis (eds.) *Large-scale neuronal theories of the brain*, Cambridge, MIT Press.

Mignard, M. and Malpeli, J. (1991). Paths of information flow through visual cortex. *Science*, **251**, 1249-1251.

Parent, P. and Zucker, S. (1989). Trace inference, curvature consistency, and curve detection. *IEEE Trans. PAMI*, **11**, 823-839.

Peterhans, E. and von der Heydt, R. (1989). Mechanisms of contour perception in monkey visual cortex. II. Contours bridging gaps. *J. of Neurosci.*, **9**, 1749-1763.

Peterhans, E. and von der Heydt, R. (1991). Subjective contours – bridging the gap between psychophysics and physiology. *Trends in Neurosci.*, **14**, 112-119.

Polat, U. and Sagi, D. (1994). The architecture of perceptual spatial interactions. *Vis. Res.*, **34**, 73-78.

Prazdny, K. (1983). Illusory contours are not caused by simultaneous contrast. *Perc. and Psychophys.*, **34**, 403-404.

Prazdny, K. (1984). On the perception of Glass patterns. *Perception*, **13**, 469-478.

Prazdny, K. (1986). Psychophysical and computatinal studies of random-dot Moire patterns. *Spatial Vis.*, **1**, 231-242.

Press, W.H., Flannery, B.P., Teukolsky, S.A., and Vetterling, W.T. (1989). Numerical Recipes in C/Fortran/Pascal. Cambridge Univ. Press, New York.

Rao, R.P.N. and Ballard, D.H. (1996). The visual cortex as a hierarchical predictor. Univ. of Rochester, Dept. of Computer Science, TR 96.4

Rao, R.P.N. and Ballard, D.H. (1997). Dynamic model of visual recognition predicts neural response properties in the visual cortex. *Neural Comp.*, **9**, 721-763.

Rieger, J. and Gegenfurtner, K. (1998). Temporal dynamics of contrast sensitivity and contour interpolation in illusory figures. (submitted).

Ringach, D.L., Hawken, M.J., and Shapley, R. (1997). Dynamics of orientation tuning in macaque primary visual cortex. *Nature*, **387**, 281-284.

Rockland, K. and Virga, A. (1989). Terminal arbors of individual "feedback" axons projecting from area V2 to V1 in the macaque monkey: A study using immunohistochemistry of anterogradely transported Phaseolus vulgaris-lencoagglunitin. *J. of Comp. Neurol.*, **285**, 54-72.

Sagi, D. and Kovácz, I. (1993). Long range processes involved in the perception of Glass patterns. *Inv. Ophthal. Vis. Science*, **34**(4), 1130 (PGM #2106).

Salin, P.-A. and Bullier, J. (1995). Corticocortical connections in the visual system: Structure and function. *Physiol. Rev.*, **75**, 107-154.

Sandell, J. and Schiller, P. (1982). Effect of cooling area 18 on striate cortex cells in the squirrel monkey. *J. of Neurophys.*, **48**, 38-48.

Shipley, T.F. and Kellman, P.J. (1990). The role of discontinuities in the perception of subjective figures. *Perc. and Psychophys.*, **48**, 259-270.

Shipley, T.F. and Kellman, P.J. (1992). Strength of visual interpolation depends on the ratio of physically specified to total edge length. *Perc. and Psychophys.*, **52**, 97-106.

Smits, J.T.S., Vos, P.G., and van Oeffelen, M.P. (1985). The perception of a dotted line in noise: A model of good continuation and some experimental results. *Spatial Vis.*, **1**, 163-177.

Tononi, G., Sporns, O., and Edelman, G.M. (1992). Reentry and the problem of integrating multiple cortical areas: Simulation of dynamic integration in the visual system. *Cerebral Cortex*, **2**, 310-335.

Ullman, S. (1995). Sequence seeking and counter streams: A computational model for bidirectional information flow in the visual cortex. *Cerebral Cortex*, **1**, 1-11.

von der Heydt, R., Peterhans, E., and Baumgartner, G. (1984). Illusory contours and cortical neuron responses. *Science*, **224**, 1260-1262.

von der Heydt, R., Heitger, F., and Peterhans, E. (1993). Perception of occluding contours: Neural mechanisms and a computational model. *Biomed. Res.*, **14**, 1-6.

von der Heydt, R. and Peterhans, E. (1989). Mechanisms of contour perception in monkey visual cortex. I. Lines of pattern discontinuity. *J. Neurosci.*, **9**, 1731-1748.

Zipser, K., Lamme, V.A.F., and Schiller, P.H. (1996). Contextual modulation in primary visual cortex. *J. Neurosci.*, **15**, 7376-7389.

Zipser, K., Lamme, V.A.F., and Spekreijse, H. (1997). Figure-ground signals in V1 eliminated by anaesthesia. *Inv. Ophthal. Vis. Science*, **38**(4), S969 (PGM #4491).

Zucker, S. (1985). Early orientation selection: Tangent fields and the dimensionality of their support. *Comp. Vis., Graph., and Image Process.*, **32**, 74-103.

Appendix 1: Properties of the Gain Control Mechanism

We investigate the enhancement and reduction of responses via the top-down feedback scheme depending on the structure of the input configuration. In particular, we analyze the modification of an activation at a target location for one selected orientation by way of the top-down gain control mechanism. Three idealized cases will be considered: *(i)* the transformation of an isolated activity for a given orientation, *(ii)* conditions for the enhancement of a localized activity that is supported by an arrangement of colinear activation, and *(iii)* conditions for the reduction of an activation that is embedded in a dense field of co-oriented activities in a spatial neighborhood. For all input configurations, we assume unit input activation at each discrete spatial location. Since we particularly investigate one orientation field of input activation we can neglect any cross-orientation interactions. We therefore simplify the following derivations by taking a unit weighting for the orientation fields, $\Psi^{-}_{00} = 1$.

In the first experiment, we assume a localized input activation of unit magnitude for one orientation. This setup is defined by

$$c_{i'\tau} = \begin{cases} 1 & \text{for } \tau = \theta \wedge i' = i \\ 0 & \text{for } \tau \neq \theta \vee i' \neq i \end{cases}$$

In this case no feedback activation $h^{(2)}_{i\theta}$ is generated. We get the steady-state response of Eqn. 1

$$l^{(1)}_{i\theta} = \frac{\beta_1}{\alpha_1}.$$

The $l^{(1)}_{i\theta}$ response is just a scaled version of the input. We use this level as a reference to find conditions to achieve the desired functionality of enhancement and reduction of initial responses.

In the second case the initial response is supplied by two colinear flanking activations located at positions $i' = i \pm \Delta$. This input configuration initiates a response at the stage of model V2 which in turn generates a feedback signal. This feedback activation defines the gain for enhancement of the activity at the target location. The top-down activation also contributes an inhibitory component which, in this configuration, is scaled by the connection strength at the center of the spatial weighting function Λ_{00}. We find the steady-state response

$$l^{(1)}_{i\theta} = \frac{\beta_1 \left(1 + C h^{(2)}_{i\theta}\right)}{\alpha_1 + \zeta_1 \Lambda^{-}_{00} h^{(2)}_{i\theta}}.$$

In the colinear arrangement the initial activation should be strengthened in comparison to the case of having only an isolated input activity. We find the condition for enhancement of initial response

via top-down gating by

$$C > \frac{\zeta_1}{\alpha_1} \cdot \Lambda_{00}^{-}.$$

The third case consists of a dense field of equally oriented unit amplitude input activations. Again, we find the steady-state response

$$l_{i\theta}^{(1)} = \frac{\beta_1 \left(1 + C h_{i\theta}^{(2)}\right)}{\alpha_1 + \zeta_1 h_{i\theta}^{(2)}}.$$

The response thus differs to the second condition only by an increased inhibitory contribution from the dense field of like-oriented activities. In this case now, we want to achieve a reduction of response relative to the isolated input considered in the first case. We find the corresponding condition for reduction of initial response via top-down interaction by

$$C < \frac{\zeta_1}{\alpha_1}.$$

Appendix 2: Weighting Functions of 'Contour Templates'

The connectivity patterns of the weighting functions consist of an ON- as well as an OFF-subfield for each lobe of the bipole, $\Gamma_{i\theta}^{\pm,L}$ and $\Gamma_{i\theta}^{\pm,R}$. The excitatory ON-connectivity is defined for 'relatable' orientations. Kellman and Shipley (1991) defined 'relatability' for tangent orientations to be interpolated by a smooth curve which *(a)* contains no inflection point and *(b)* does not bend to form an acute angle. Thus, we find a range of $\theta + \alpha \leq \phi^{+} < \theta + \frac{\pi}{2}$ to be relatable at location Q. We define maximum support for contrast responses in a cocircular arrangement (Zucker, 1985; Parent and Zucker, 1989). Figure 7 (left, top) sketches the geometric arrangement of a cocircular contrast orientation at Q that is supportive for the activation at P along θ. Maximum ON-connectivity is given for cocircular arrangements at $\phi^{+} = \theta + 2\alpha$ with $\alpha = \tan^{-1}(\frac{y_Q - y_P}{x_Q - x_P})$ (Fig. 7, right, top). Non-relatable orientations define the OFF-connectivity in the 'contour templates'. The maximum inhibitory weighting is defined for $\phi^{-} = \theta$ (Fig. 7, right, bottom). We center Gaussian weighting functions at the orientations of maximum excitatory and inhibitory strength, respectively, and define a localized excitatory influence together with a more broad inhibitory weighting, $\sigma_{\Psi}^{+} < \sigma_{\Psi}^{-}$.

The elongated spatial weighting function of 'contour templates' is assembled by two subfields. The integration of curved structure in a smaller neighorhood as well as straight oriented contrast along a longer range is supplied. Each subfield weighting function can be synthesized by the superposition of an ellipse with a circle that is shifted to either end of the ellipse (Fig. 7, left, bottom). The resulting outline contours of the spatial weighting functions are defined to follow the shape of a Poisson distribution along the axis of elongation.

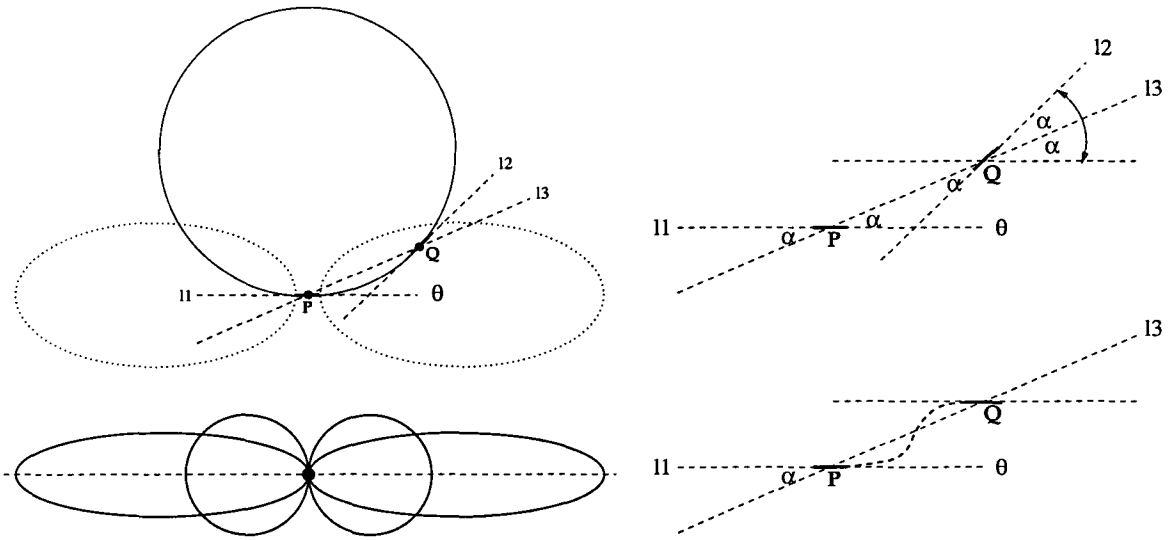

Figure 7: *Structure of bipole 'contour templates'. Left: Contour cell at position P with orientation θ; for a given location Q in the spatial neighborhood of the target cell (dashed ellipses) the orientation that is maximally 'relatable' is defined by the tangent orientation in Q of the osculating circle which passes through P and Q and is tangent to θ (top). The spatial weighting functions for the subfields are described by superimposed ellipses with shifted circular weightings (bottom). Right: Tangent orientations for a cocircular arrangement of contrast responses that define excitatory weights in the* ON*-subfield (top). Straight line l1 defines the orientation axis of the contour cell at P, line l3 denotes the virtual line connecting locations P and Q, and line l2 denotes the tangent orientations that are 'relatable' and give maximum support for $\phi = \theta + 2\alpha$. The* OFF*-subfield defines inhibitory connections for those orientations that are not 'relatable' (bottom).*

Appendix 3: V2 Contour Cell Responses

The accumulation of normalized $l^{(2)}_{i\theta}$-activities is accomplished by a micro-circuit of feedforward interaction. This circuit is designed such that an oriented V2 contour cell only gets activated if significant input is available from *both* branches of an elongated bipartite RF (see Eqn. 2, center and right). Superscripts + and − identify the individual ON- and OFF-subfield weighting functions for the segregated left and right branch of a 'curvature template'. The weighted integration of activities in space/orientation domain is a linear process. Thus, we superimpose the ON- and OFF-weights by taking their difference. The single space/orientation weighting functions for left and right branches are then convolved against the normalized activity distribution of initial contrast responses. Negative responses are rectified. We get

$$\begin{aligned} v^L_{i\theta} &= \max\left[\left\{l^{(2)} \star \left(\Gamma^{+,L} - \Gamma^{-,L}\right)\right\}_{i\theta}, 0\right], \quad \text{and} \\ v^R_{i\theta} &= \max\left[\left\{l^{(2)} \star \left(\Gamma^{+,R} - \Gamma^{-,R}\right)\right\}_{i\theta}, 0\right]. \end{aligned}$$

These activations are fed forward to the internal stages of the micro-circuit (see Fig. 2, center). The stages of the circuit at $q^L_{i\theta}$ and $q^R_{i\theta}$, respectively, combine the activities from both bipole lobes in a cross-inhibitory fashion. We assume that the individual cell responses equilibrate fast such that we can utilize steady-state activities. In particular, for the cross-inhibition between left and right branches we have

$$q^L_{i\theta} = \frac{v^L_{i\theta}}{1 + \zeta_3 v^R_{i\theta}}, \quad \text{and} \quad q^R_{i\theta} = \frac{v^R_{i\theta}}{1 + \zeta_3 v^L_{i\theta}},$$

where ζ_3 defines the gain of the shunting inhibitory interaction. The next stage realizes the self-inihibition of each lobe which is disinhibited if both branches are active. We get

$$r^L_{i\theta} = v^L_{i\theta} - q^L_{i\theta}, \quad \text{and} \quad r^R_{i\theta} = v^R_{i\theta} - q^R_{i\theta}.$$

Final pooling of equilibrated responses from individual input branches results in

$$h^{(1)}_{i\theta} = r^L_{i\theta} + r^R_{i\theta}.$$

Consider the case that activity is contributed by only one branch, say the left one, activities at the first stage can be easily calculated as $q^L_{i\theta} = v^L_{i\theta}$ and $q^R_{i\theta} = 0$. Self-inhibition in turn causes activities $r^L_{i\theta} = r^R_{i\theta} = 0$ such that the target contour cell remains inactivated. The micro-circuit implements the functionality of an AND-gate in which both lobes of the 'contour template' must be activated in order to generate a contour cell response. If we lump together the individual stages, the final $h^{(1)}_{i\theta}$ equilibrium response of the non-linear circuit results in (see Eqn. 3)

$$h^{(1)}_{i\theta} = v^L_{i\theta} v^R_{i\theta} \frac{\frac{2}{\zeta_3} + v^L_{i\theta} + v^R_{i\theta}}{\frac{1}{\zeta_3{}^2} + \frac{1}{\zeta_3}\left(v^L_{i\theta} + v^R_{i\theta}\right) + v^L_{i\theta} v^R_{i\theta}}. \tag{6}$$

The activities of both lobes effectively combine in a multiplicative fashion. Parameter ζ_3 determines the shape of the non-linear transfer function to compress the input activation and therefore determines the responsiveness according to any graded V1 contrast input. Investigating the individual stages of the micro-circuit, we directly observe that a parameter setting $\zeta_3 = 0$ will eliminate the disinhibitory effect and, as a consequence, virtually inactivates the opposite lobe. As a result, contour cells will never respond. Increasing values of ζ_3 increase the disinhibitory effect of cross-channel interaction. We investigate those cases in which $\zeta_3 v^R_{i\theta} \gg 1$ and $\zeta_3 v^L_{i\theta} \gg 1$ where input configurations generate a strong cross-inhibition effect. We get $q^L_{i\theta} \approx v^L_{i\theta}/(\zeta_3 v^R_{i\theta})$ and $q^R_{i\theta} \approx v^R_{i\theta}/(\zeta_3 v^L_{i\theta})$, respectively. With *both* lobes receiving input activation we have

$$h^{(1)}_{i\theta} = v^L_{i\theta} + v^R_{i\theta} - \frac{1}{\zeta_3}\left(\frac{v^L_{i\theta}}{v^R_{i\theta}} + \frac{v^R_{i\theta}}{v^L_{i\theta}}\right). \tag{7}$$

Taking the limit $\zeta_3 \rightarrow \infty$ Eqn. 7 demonstrates that the inhibitory component vanishes such that the upper limit of contour cell response is determined by the sum of inputs from both subfield branches. We define the average input $\bar{v}_{i\theta} = (v_{i\theta}^L + v_{i\theta}^R)/2$. Any imbalanced input is defined relative to the constant average, such that $v_{i\theta}^L = (1-k)\bar{v}_{i\theta}$ and $v_{i\theta}^L = (1+k)\bar{v}_{i\theta}$ $(0 \leq k < 1)$. The contour cell response can now be rewritten as (see Eqn. 4)

$$h_{i\theta}^{(1)}(k) = 2\bar{v}_{i\theta} - \frac{1}{\zeta_3} \cdot \frac{1+2k^2}{1-k^2}.$$

We get equal input magnitudes from both branches for $k = 0$. For increasing values of k we get monotonically increasing reduction of contour responses. This shows that contour cell responses are selective to the imbalance of input amplitudes from both branches. Such an imbalance can be used as a measure of structural (in)coherence in the input configuration. Equation 6 further demonstrates how contour cell responses vary for scaled contrast cell inputs. We define $v_{i\theta}^{L^*} = m \cdot v_{i\theta}^L$ and $v_{i\theta}^{R^*} = m \cdot v_{i\theta}^R$ and further assume $\zeta_3{}^* = m^{-1}\zeta_3$ (m is a scaling constant). The resulting contour cell response is scaled by the same factor m. This demonstrates that if we want to retain the functionality of the bipole integration scheme for scaled average input we have to inversely scale the gain parameter for controlling the shunting cross-inhibition.

Appendix 4: Model Parameters

The following tables display the network equations of the model. All parameter settings that have been used in all computational experiments are presented. We split the summary into two separate parts, showing equations and settings for model V1 and V2, respectively.

$l_{i\theta}^{(1)}$	Brief description	Gain control via top-down activation and feedback competition
	Activation dynamics	$\frac{\partial}{\partial t} l_{i\theta}^{(1)} = -\alpha_1 l_{i\theta}^{(1)} + \beta_1 c_{i\theta} \left(1 + C \left\{h^{(2)} \star \Psi^{+}\right\}_{i\theta}\right) - \zeta_1 l_{i\theta}^{(1)} \left\{h^{(2)} \star \Psi^{-} \star \Lambda^{-}\right\}_{i\theta}$
	Parameter settings	Shunting interaction: $\alpha_1 = 1\,, \quad \beta_1 = 0.42\,, \quad \zeta_1 = 13$ Top-down gain factor: $C = 5$ ($C = 10$, Fig.4) Weightings: Λ: $\sigma_{\Lambda}^{-} = 1.8$; Ψ: $\sigma_{\Psi}^{+} = 0.7\,, \quad \sigma_{\Psi}^{-} = 2.5$
$l_{i\theta}^{(2)}$	Brief description	Contrast enhancement and activity normalization via space/orientation competition
	Equilibrium response	$l_{i\theta}^{(2)} = \frac{\beta_2 l_{i\theta}^{(1)} - \delta_2 \left\{l^{(1)} \star \Psi^{-} \star \Lambda^{-}\right\}_{i\theta}}{\alpha_2 + \zeta_2 \left\{l^{(1)} \star \Psi^{-} \star \Lambda^{-}\right\}_{i\theta}}$
	Parameter settings	Shunting interaction: $\alpha_2 = 1\,, \quad \beta_2 = 4\,, \quad \delta_2 = 4\,, \quad \zeta_2 = 10$ Weightings: Λ: $\sigma_{\Lambda}^{-} = 1.3$; Ψ: $\sigma_{\Psi}^{-} = 2.5$

Table 1: Summary of equations and parameter settings for model area V1.

$h_{i\theta}^{(1)}$	Brief description	Compatibility and weighting function for the bipole 'curvature template'
	Activation (final output)	$h_{i\theta}^{(1)} = v_{i\theta}^{L} v_{i\theta}^{R} \frac{\frac{2}{\zeta_3} + v_{i\theta}^{L} + v_{i\theta}^{R}}{\frac{1}{\zeta_3^2} + \frac{1}{\zeta_3}\left(v_{i\theta}^{L} + v_{i\theta}^{R}\right) + v_{i\theta}^{L} v_{i\theta}^{R}}$
	Parameters	Shunting interaction (micro-circuit): $\zeta_3 = 15$ Spatial weightings: Γ_{Λ}^{elong}: $\sigma_{elong} = 8.0\,, \quad \sigma_{orth} = 1.0$; Γ_{Λ}^{circ}: $\sigma_{rad} = 2.0$ Relatability: Γ_{Ψ}: $\sigma_{\Psi}^{+} = 1.0\,, \quad \sigma_{\Psi}^{-} = 1.6$
$h_{i\theta}^{(2)}$	Brief description	Contrast enhancement and activity normalization by space/orientation competition
	Equilibrium response	$h_{i\theta}^{(2)} = \frac{\beta_4 h_{i\theta}^{(1)} - \delta_4 \left\{h_{i\theta}^{(1)} \star \Psi^{-} \star \Lambda^{-}\right\}_{i\theta}}{\alpha_4 + \zeta_4 \left\{h_{i\theta}^{(1)} \star \Psi^{-} \star \Lambda^{-}\right\}_{i\theta}}$
	Parameter settings	Shunting interaction: $\alpha_4 = 1.6\,, \quad \beta_4 = 14\,, \quad \delta_4 = 12\,, \quad \zeta_4 = 32$ Weightings: Λ: $\sigma_{\Lambda}^{-} = 1.6$; Ψ: $\sigma_{\Psi}^{-} = 0.5$

Table 2: *Summary of equations and parameter settings for model area V2.*

Liste der bisher erschienenen Ulmer Informatik-Berichte

Einige davon sind per FTP von `ftp.informatik.uni-ulm.de` erhältlich
Die mit * markierten Berichte sind vergriffen

List of technical reports published by the University of Ulm

Some of them are available by FTP from `ftp.informatik.uni-ulm.de`
Reports marked with * are out of print

91-01 *Ker-I Ko, P. Orponen, U. Schöning, O. Watanabe*
Instance Complexity

91-02* *K. Gladitz, H. Fassbender, H. Vogler*
Compiler-Based Implementation of Syntax-Directed Functional Programming

91-03* *Alfons Geser*
Relative Termination

91-04* *J. Köbler, U. Schöning, J. Toran*
Graph Isomorphism is low for PP

91-05 *Johannes Köbler, Thomas Thierauf*
Complexity Restricted Advice Functions

91-06* *Uwe Schöning*
Recent Highlights in Structural Complexity Theory

91-07* *F. Green, J. Köbler, J. Toran*
The Power of Middle Bit

91-08* *V.Arvind, Y. Han, L. Hamachandra, J. Köbler, A. Lozano, M. Mundhenk, A. Ogiwara, U. Schöning, R. Silvestri, T. Thierauf*
Reductions for Sets of Low Information Content

92-01* *Vikraman Arvind, Johannes Köbler, Martin Mundhenk*
On Bounded Truth-Table and Conjunctive Reductions to Sparse and Tally Sets

92-02* *Thomas Noll, Heiko Vogler*
Top-down Parsing with Simulataneous Evaluationof Noncircular Attribute Grammars

92-03 *Fakultät für Informatik*
17. Workshop über Komplexitätstheorie, effiziente Algorithmen und Datenstrukturen

92-04* *V. Arvind, J. Köbler, M. Mundhenk*
Lowness and the Complexity of Sparse and Tally Descriptions

92-05* *Johannes Köbler*
Locating P/poly Optimally in the Extended Low Hierarchy

92-06* *Armin Kühnemann, Heiko Vogler*
Synthesized and inherited functions -a new computational model for syntax-directed semantics

92-07* *Heinz Fassbender, Heiko Vogler*
A Universal Unification Algorithm Based on Unification-Driven Leftmost Outermost Narrowing

92-08* *Uwe Schöning*
On Random Reductions from Sparse Sets to Tally Sets

92-09* *Hermann von Hasseln, Laura Martignon*
Consistency in Stochastic Network

92-10 *Michael Schmitt*
A Slightly Improved Upper Bound on the Size of Weights Sufficient to Represent Any Linearly Separable Boolean Function

92-11 *Johannes Köbler, Seinosuke Toda*
On the Power of Generalized MOD-Classes

92-12 *V. Arvind, J. Köbler, M. Mundhenk*
Reliable Reductions, High Sets and Low Sets

92-13 *Alfons Geser*
On a monotonic semantic path ordering

92-14* *Joost Engelfriet, Heiko Vogler*
The Translation Power of Top-Down Tree-To-Graph Transducers

93-01 *Alfred Lupper, Konrad Froitzheim*
AppleTalk Link Access Protocol basierend auf dem Abstract Personal Communications Manager

93-02 *M.H. Scholl, C. Laasch, C. Rich, H.-J. Schek, M. Tresch*
The COCOON Object Model

93-03 *Thomas Thierauf, Seinosuke Toda, Osamu Watanabe*
On Sets Bounded Truth-Table Reducible to P-selective Sets

93-04 *Jin-Yi Cai, Frederic Green, Thomas Thierauf*
On the Correlation of Symmetric Functions

93-05 *K.Kuhn, M.Reichert, M. Nathe, T. Beuter, C. Heinlein, P. Dadam*
A Conceptual Approach to an Open Hospital Information System

93-06 *Klaus Ganer*
Rechnerunterstttzung fr die konzeptuelle Modellierung

93-07 *Ullrich Keler, Peter Dadam*
Towards Customizable, Flexible Storage Structures for Complex Objects

94-01 *Michael Schmitt*
On the Complexity of Consistency Problems for Neurons with Binary Weights

94-02 *Armin Khnemann, Heiko Vogler*
A Pumping Lemma for Output Languages of Attributed Tree Transducers

94-03 *Harry Buhrman, Jim Kadin, Thomas Thierauf*
On Functions Computable with Nonadaptive Queries to NP

94-04 *Heinz Faßbender, Heiko Vogler, Andrea Wedel*
Implementation of a Deterministic Partial E-Unification Algorithm for Macro Tree Transducers

94-05 *V. Arvind, J. Köbler, R. Schuler*
On Helping and Interactive Proof Systems

94-06 *Christian Kalus, Peter Dadam*
Incorporating record subtyping into a relational data model

94-07 *Markus Tresch, Marc H. Scholl*
A Classification of Multi-Database Languages

94-08 *Friedrich von Henke, Harald Rueß*
Arbeitstreffen Typtheorie: Zusammenfassung der Beiträge

94-09 *F.W. von Henke, A. Dold, H. Rueß, D. Schwier, M. Strecker*
Construction and Deduction Methods for the Formal Development of Software

94-10 *Axel Dold*
Formalisierung schematischer Algorithmen

94-11 *Johannes Köbler, Osamu Watanabe*
New Collapse Consequences of NP Having Small Circuits

94-12 *Rainer Schuler*
On Average Polynomial Time

94-13 *Rainer Schuler, Osamu Watanabe*
Towards Average-Case Complexity Analysis of NP Optimization Problems

94-14 *Wolfram Schulte, Ton Vullinghs*
Linking Reactive Software to the X-Window System

94-15 *Alfred Lupper*
Namensverwaltung und Adressierung in Distributed Shared Memory-Systemen

94-16 *Robert Regn*
Verteilte Unix-Betriebssysteme

94-17 *Helmuth Partsch*
Again on Recognition and Parsing of Context-Free Grammars:
Two Exercises in Transformational Programming

94-18 *Helmuth Partsch*
Transformational Development of Data-Parallel Algorithms: an Example

95-01 *Oleg Verbitsky*
On the Largest Common Subgraph Problem

95-02 *Uwe Schöning*
Complexity of Presburger Arithmetic with Fixed Quantifier Dimension

95-03 *Harry Buhrman, Thomas Thierauf*
The Complexity of Generating and Checking Proofs of Membership

95-04 *Rainer Schuler, Tomoyuki Yamakami*
Structural Average Case Complexity

95-05 *Klaus Achatz, Wolfram Schulte*
Architecture Indepentent Massive Parallelization of Divide-And-Conquer Algorithms

95-06 *Christoph Karg, Rainer Schuler*
Structure in Average Case Complexity

95-07 *P. Dadam, K. Kuhn, M. Reichert, T. Beuter, M. Nathe*
ADEPT: Ein integrierender Ansatz zur Entwicklung flexibler, zuverlässiger kooperierender Assistenzsysteme in klinischen Anwendungsumgebungen

95-08 *Jürgen Kehrer, Peter Schulthess*
Aufbereitung von gescannten Röntgenbildern zur filmlosen Diagnostik

95-09 *Hans-Jörg Burtschick, Wolfgang Lindner*
On Sets Turing Reducible to P-Selective Sets

95-10 *Boris Hartmann*
Berücksichtigung lokaler Randbedingung bei globaler Zieloptimierung mit neuronalen Netzen am Beispiel Truck Backer-Upper

95-12 *Klaus Achatz, Wolfram Schulte*
Massive Parallelization of Divide-and-Conquer Algorithms over Powerlists

95-13 *Andrea Mößle, Heiko Vogler*
Efficient Call-by-value Evaluation Strategy of Primitive Recursive Program Schemes

95-14 *Axel Dold, Friedrich W. von Henke, Holger Pfeifer, Harald Rueß*
A Generic Specification for Verifying Peephole Optimizations

96-01 *Ercüment Canver, Jan-Tecker Gayen, Adam Moik*
Formale Entwicklung der Steuerungssoftware für eine elektrisch ortsbediente Weiche mit VSE

96-02 *Bernhard Nebel*
Solving Hard Qualitative Temporal Reasoning Problems: Evaluating the Efficiency of Using the ORD-Horn Class

96-03 *Ton Vullinghs, Wolfram Schulte, Thilo Schwinn*
An Introduction to TkGofer

96-04 *Thomas Beuter, Peter Dadam*
Anwendungsspezifische Anforderungen an Workflow-Mangement-Systeme am Beispiel der Domäne Concurrent-Engineering

96-05 *Gerhard Schellhorn, Wolfgang Ahrendt*
Verification of a Prolog Compiler - First Steps with KIV

96-06 *Manindra Agrawal, Thomas Thierauf*
Satisfiability Problems

96-07 *Vikraman Arvind, Jacobo Torán*
A nonadaptive NC Checker for Permutation Group Intersection

96-08 *David Cyrluk, Oliver Möller, Harald Rueß*
An Efficient Decision Procedure for a Theory of Fix-Sized Bitvectors with Composition and Extraction

96-09 *Bernd Biechele, Dietmar Ernst, Frank Houdek, Joachim Schmid, Wolfram Schulte*
Erfahrungen bei der Modellierung eingebetteter Systeme mit verschiedenen SA/RT–Ansätzen

96-10 *Falk Bartels, Axel Dold, Friedrich W. von Henke, Holger Pfeifer, Harald Rueß*
Formalizing Fixed-Point Theory in PVS

96-11 *Axel Dold, Friedrich W. von Henke, Holger Pfeifer, Harald Rueß*
Mechanized Semantics of Simple Imperative Programming Constructs

96-12 *Axel Dold, Friedrich W. von Henke, Holger Pfeifer, Harald Rueß*
Generic Compilation Schemes for Simple Programming Constructs

96-13 *Klaus Achatz, Helmuth Partsch*
From Descriptive Specifications to Operational ones: A Powerful Transformation Rule, its Applications and Variants

97-01 *Jochen Messner*
Pattern Matching in Trace Monoids

97-02 *Wolfgang Lindner, Rainer Schuler*
A Small Span Theorem within P

97-03 *Thomas Bauer, Peter Dadam*
A Distributed Execution Environment for Large-Scale Workflow Management Systems with Subnets and Server Migration

97-04 *Christian Heinlein, Peter Dadam*
Interaction Expressions - A Powerful Formalism for Describing Inter-Workflow Dependencies

97-05 *Vikraman Arvind, Johannes Köbler*
On Pseudorandomness and Resource-Bounded Measure

97-06 *Gerhard Partsch*
Punkt-zu-Punkt- und Mehrpunkt-basierende LAN-Integrationsstrategien
für den digitalen Mobilfunkstandard DECT

97-07 *Manfred Reichert, Peter Dadam*
$ADEPT_{flex}$ - Supporting Dynamic Changes of Workflows Without Loosing Control

97-08 *Hans Braxmeier, Dietmar Ernst, Andrea Mößle, Heiko Vogler*
The Project NoName - A functional programming language with its development environment

97-09 *Christian Heinlein*
Grundlagen von Interaktionsausdrücken

97-10 *Christian Heinlein*
Graphische Repräsentation von Interaktionsausdrücken

97-11 *Christian Heinlein*
Sprachtheoretische Semantik von Interaktionsausdrücken

97-12 *Gerhard Schellhorn, Wolfgang Reif*
Proving Properties of Finite Enumerations: A Problem Set for Automated Theorem Provers

97-13 *Dietmar Ernst, Frank Houdek, Wolfram Schulte, Thilo Schwinn*
Experimenteller Vergleich statischer und dynamischer Softwareprüfung für eingebettete Systeme

97-14 *Wolfgang Reif, Gerhard Schellhorn*
Theorem Proving in Large Theories

97-15 *Thomas Wennekers*
Asymptotik rekurrenter neuronaler Netze mit zufälligen Kopplungen

97-16 *Peter Dadam, Klaus Kuhn, Manfred Reichert*
Clinical Workflows - The Killer Application for Process-oriented Information Systems?

97-17 *Mohammad Ali Livani, Jörg Kaiser*
EDF Consensus on CAN Bus Access in Dynamic Real-Time Applications

97-18 *Johannes Köbler,Rainer Schuler*
Using Efficient Average-Case Algorithms to Collapse Worst-Case Complexity Classes

98-01 *Daniela Damm, Lutz Claes, Friedrich W. von Henke, Alexander Seitz, Adelinde Uhrmacher, Steffen Wolf*
Ein fallbasiertes System für die Interpretation von Literatur zur Knochenheilung

98-02 *Thomas Bauer, Peter Dadam*
Architekturen für skalierbare Workflow-Management-Systeme - Klassifikation und Analyse

98-03 *Marko Luther, Martin Strecker*
A guided tour through *Typelab*

98-04 *Heiko Neumann, Luiz Pessoa*
Visual Filling-in and Surface Property Reconstruction

98-05 *Ercüment Canver*
Formal Verification of a Coordinated Atomic Action Based Design

98-06 *Andreas Küchler*
On the Correspondence between Neural Folding Architectures and Tree Automata

98-07 *Heiko Neumann, Thorsten Hansen, Luiz Pessoa*
Interaction of ON and OFF Pathways for Visual Contrast Measurement

98-08 *Thomas Wennekers*
Synfire Graphs: From Spike Patterns to Automata of Spiking Neurons

98-09 *Thomas Bauer, Peter Dadam*
Variable Migration von Workflows in *ADEPT*

98-10 *Heiko Neumann, Wolfgang Sepp*
Recurrent V1 – V2 Interaction in Early Visual Boundary Processing

Ulmer Informatik-Berichte

ISSN 0939-5091

Herausgeber: Fakultät für Informatik

Universität Ulm, Oberer Eselsberg, D-89069

Ulm